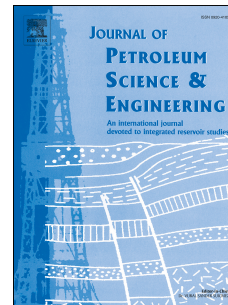


Accepted Manuscript

Development of inflow performance model in high temperature gas-condensate reservoirs

Foad Faraji, Johnson Ugwu, Farhad Nabhani, Perk C. Lin



PII: S0920-4105(19)30581-9

DOI: <https://doi.org/10.1016/j.petrol.2019.06.033>

Reference: PETROL 6169

To appear in: *Journal of Petroleum Science and Engineering*

Received Date: 31 December 2018

Revised Date: 19 May 2019

Accepted Date: 11 June 2019

Please cite this article as: Faraji, F., Ugwu, J., Nabhani, F., Lin, P.C., Development of inflow performance model in high temperature gas-condensate reservoirs, *Journal of Petroleum Science and Engineering* (2019), doi: <https://doi.org/10.1016/j.petrol.2019.06.033>.

This is a PDF file of an unedited manuscript that has been accepted for publication. As a service to our customers we are providing this early version of the manuscript. The manuscript will undergo copyediting, typesetting, and review of the resulting proof before it is published in its final form. Please note that during the production process errors may be discovered which could affect the content, and all legal disclaimers that apply to the journal pertain.

Development of Inflow Performance Model in High Temperature Gas-Condensate Reservoirs

Abstract

Inflow Performance Relationships (IPRs) are important element for reservoir engineers in the design of new wells and also for monitoring and optimizing existing wells. IPRs are used to determine optimum production of gas rate and condensate rate in a well for any specified value of average reservoir pressure and predict the performance.

Jokhio and Tiab proposed a simple method of establishing IPR for gas condensate wells. The method uses transient pressure test data to estimate effective permeability as a function of pressure. Effective permeability data used to convert production bottomhole flow pressure into pseudopressure to establish well performance. Despite the effectiveness of the method, single phase correlations were used in PVT calculations of each phase, which over simplified the fluid flow in gas condensate wells. Single phase dry gas equations do not reflect the multiphase flow behaviour of gas condensate wells below the dew point. Due to this limitation Jokhio and Tiab method modified by this study and new analytical IPRs for gas condensate well proposed.

The major improvement of the above method is incorporating new viscosity correlation developed by this study and using two-phase compressibility factor as key parameters for predicting gas condensate inflow performance. Therefore, the main contribution of this study is development of viscosity correlation which is a critical issue in predicting gas condensate inflow performance both above and below the dew point. Optimization techniques and nonlinear regression used to develop a new viscosity correlation for high temperature heavy gas condensate reservoirs under depletion.

The application of the new model is illustrated with field example for current IPR curves. Compositional simulation study of the well performed in PIPSIM simulator. The proposal approach provides reasonable estimates of simulator input reservoir properties (e.g. IPRs). Accuracy of the new method compared with compositional simulation study. The proposed method presents average absolute relative deviation (AARD) of 5.8% for gas IPR and 7.5% for condensate IPR compare to compositional simulation results. New method provides a tool for quick estimation of gas condensate wells without need of relative permeability curves and expensive and time consuming compositional simulation.

Keywords

Inflow Performance Relationship (IPR); Gas Condensate Reservoirs; Viscosity, two phase Compressibility Factor, analytical condensate well IPR, pressure build up test.

34 Nomenclature

| | | |
|----|----------|--|
| 35 | Bc | Condensate formation volume factor |
| 36 | Bg | Gas formation volume factor |
| 37 | Bgd | Dry gas formation volume factor |
| 38 | BHFP | Bottom-hole flow pressure |
| 39 | C | Productivity index |
| 40 | h | Net thickness |
| 41 | K | Absolute permeability, md |
| 42 | Krg | Gas phase relative permeability |
| 43 | Kro | Oil phase relative permeability |
| 44 | Keg | Gas phase effective permeability |
| 45 | Keo | Oil phase effective permeability |
| 46 | Mg | Gas molecular weight |
| 47 | Mo | Oil molecular weight |
| 48 | mP | Pseudo-pressure function |
| 49 | Pdew | Dew point pressure |
| 50 | Pinitial | Initial pressure of the reservoir |
| 51 | Pwf | Well flowing bottom-hole pressure |
| 52 | P* | Pressure at outer boundary of Region 1 |
| 53 | Pavg | Average reservoir pressure (psia) |
| 54 | Ppr | Pseudo reduced pressure (psia) |
| 55 | Ppc | Pseudo-critical pressure |
| 56 | q | Surface flow rate |
| 57 | R | Universal gas constant |
| 58 | Rp | Producing gas to oil ratio (scf/STB) |
| 59 | Ro | Oil to gas ratio (STB/scf) |
| 60 | Rs | Solution gas to oil ratio (scf/STB) |
| 61 | r | Radial distance |
| 62 | re | External drainage radius |
| 63 | rw | Wellbore radius |
| 64 | Rs | Solution gas to oil ratio |
| 65 | Ro | Oil to gas ratio |

| | | |
|----|-----------------|--|
| 66 | R _p | Producing gas to oil ratio |
| 67 | S | Skin factor |
| 68 | T | Reservoir temperature |
| 69 | T _{sc} | Standard condition temperature |
| 70 | T _{pr} | Pseudo reduced temperature |
| 71 | T _{pc} | Pseudo-critical temperature |
| 72 | V | Volume at reservoir condition |
| 73 | dew | Dew point |
| 74 | Y | Constant term in viscosity correlation |
| 75 | Z | Compressibility factor single phase |
| 76 | Z _{2p} | Two-phase compressibility factor |

77 **Greek Letters**

| | | |
|----|------------|-----------------------------|
| 78 | ϕ | Porosity |
| 79 | μ | Viscosity |
| 80 | μ_{od} | Dead oil viscosity |
| 81 | ρ | Density |
| 82 | σ | Gas/oil interfacial tension |
| 83 | γ_g | Gas specific gravity |

84 **Subscripts**

| | | |
|----|----|-------------------------------|
| 85 | c | Condensate |
| 86 | g | Gas |
| 87 | gt | Total gas |
| 88 | n | Exponent of gas rate equation |
| 89 | o | Oil phase |
| 90 | ot | Total oil |
| 91 | V | vertical |
| 92 | SP | Single phase |
| 93 | 2p | Two-phase |

94 1. Introduction

95 Gas condensate well behaviour is unique as it is characterized by a rapid loss of well
 96 productivity. When the bottom-hole flowing pressure (P_{wf}) drops below the dew point, a
 97 region of high condensate saturation builds up near the wellbore, resulting in reduced gas

98 permeability and lower gas deliverability (Fevang and Whitson, 1996; Jokhio et al., 2002;
99 Kniazeff and Naville, 1965; Mott, 2003). It is essential to consider effect of condensate
100 blockage in calculating well deliverability. Pseudopressure function is used in gas rate
101 equation to describe the effect of condensate blockage on well deliverability through
102 establishing Inflow Performance Relationship (IPR) curve. (Fevang and Whitson, 1996;
103 Jokhio and Tiab, 2002; Mott, 2003; Stewart, 2012).

104 Gilbert, (1954) introduced Inflow Performance Relationship (IPR) for a well. O'Dell and
105 Miller, (1955) presented the first gas rate equation using pseudopressure function (mP) to
106 describe the effect of condensate blockage. In later study Kniazeff and Naville, (1965) were
107 the first to numerically model radial gas condensate well deliverability. Gondouin et al.,
108 (1967) extended the work of Kaniazeff and Naville by performing black oil simulations,
109 showing the importance of condensate blockage and non-Darcy flow effects on
110 backpressure performance. Effect of liquid drop out on non-Darcy flow described by Yu et
111 al., (1996) using modification of condensate saturation function.

112 IPR is an important tool in understanding the reservoir/well behaviour and quantifying
113 production rate and evaluate reservoir deliverability (Fattah et al., 2014; Guo et al., 2008;
114 Mott, 2003; Stewart, 2012). Fevang and Whitson, (1996) proposed a method to model
115 deliverability of gas condensate well based on pseudopressure integral (Al-Hussainy et al.,
116 1966; Fevang and Whitson, 1996). They identified the existence of three flow regions before
117 wellbore in gas condensate reservoirs. Following Fevang and Whitson, (1996), Jokhio and
118 Tiab, (2002) utilized two-phase pseudopressure integral to study effect of condensate
119 blockage in well deliverability and establish gas condensate well IPR. In their study transient
120 pressure test data used to convert production (BHFP) data into pseudopressure and
121 establish well IPR. Despite simple and effective approach of Jokhio and Tiab, (2002), fluid
122 Pressure-Volume-Temperature (PVT) properties calculated using single dry gas equations.
123 Fluid flow near well bore region in depleted gas condensate reservoir below the dew point is
124 in the form of two phases "gas and condensate (light oil)" (Fevang and Whitson, 1996;
125 Jokhio and Tiab, 2002; Mott, 2003; Qasem et al., 2014; Rahimzadeh et al., 2016; Thomas
126 and Bennion, 2009; Whitson et al., 1999). Furthermore, gas condensate PVT properties are
127 different from natural gas and crude oil due to the compositional changes that occurs below
128 the dew point (Elsharkawy, 2006; Rayes et al., 1992; Whitson et al., 2000; Yang et al.,
129 2007). Therefore using single dry gas equations for modelling gas condensate
130 pseudopressure function (mP) is oversimplifying the calculation.

131 The objective of this study is to develop new IPR curves for better performance prediction of
132 high temperature rich gas condensate reservoirs. Therefore, for better reflection of

133 aforementioned changes below the dew point a new viscosity correlation developed, using
134 nonlinear regression analysis and optimization techniques. Two sets of experimental data of
135 Yang et al., (2007) and Al-Meshari et al., (2007) was used for developing new viscosity
136 correlation. New correlation was incorporated with two-phase compressibility factor of Rayes
137 et al., (1992) in generating PVT tables and determining pseudopressure integral. Pseudo
138 critical temperature (T_{pc}) and pressure (P_{pc}) proposed by Elsharkawy et al., (2000), which
139 developed for gas condensate reservoirs were also used to model two phase compressibility
140 factor. Transient pressure test data from high temperature heavy gas condensate well was
141 obtained from Economides et al., (1989) and utilized to generate the IPR curves. New IPRs
142 covers effect of condensate blockage near wellbore region as an important factor in reducing
143 well productivity (Behmanesh et al., 2017; Chen et al., 1995; Fevang and Whitson, 1996;
144 Gondouin et al., 1967; Jokhio and Tiab, 2002; Rahimzadeh et al., 2016).

145 The remaining section of the paper is organized as follow. Section 2 is a detail description of
146 new viscosity correlation and PVT calculation. Section 3 is explaining how the new IPR
147 model developed with new viscosity correlation and two-phase compressibility factor.
148 Section 4 shows validation of the new developed model by compositional simulation and
149 analysing the results. Section 5 is presenting the results of this study and analysing the
150 finding. Section 6 concluding overall achievement of this study.

151 2. Construction of Pressure – Volume – Temperature (PVT) relationship

152 The knowledge of PVT data such as formation volume factor, viscosity, compressibility factor
153 and solution gas to oil ratio is essential to form pseudopressure integral and construct inflow
154 performance relationship (IPR). Viscosity and compressibility factor are governing
155 parameters to model gas condensate pseudopressure integral and determine the
156 performance (Arukhe and Mason, 2012; Hernandez; et al., 2002; Whitson et al., 1999; Yang
157 et al., 2007). To emphasis the important of viscosity the research shows 1% error in
158 calculating reservoir fluid viscosity resulted in 1% error in cumulative production (Al-Meshari
159 et al., 2007; Fevang and Whitson, 1996; Hernandez; et al., 2002; Sutton, 2005; Whitson et
160 al., 1999).

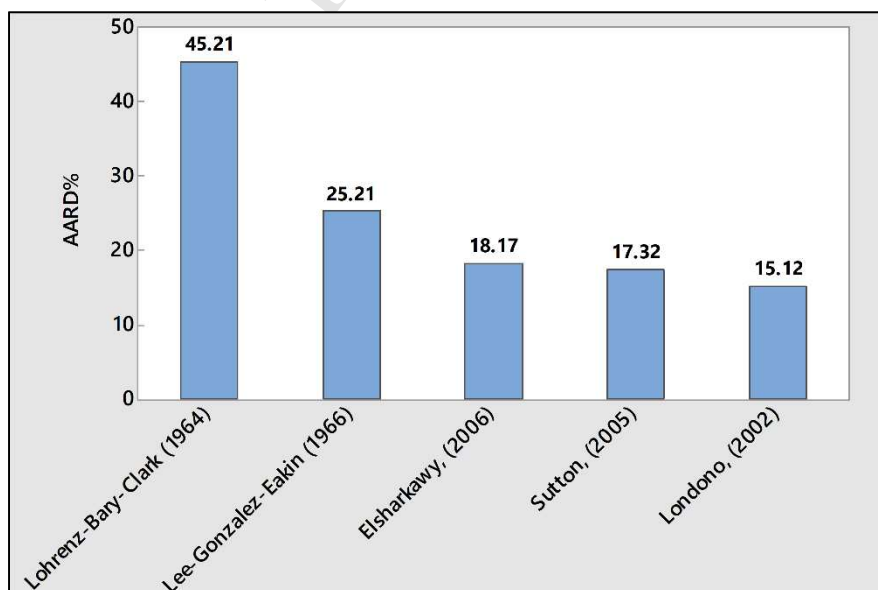
161 Behmanesh et al., (2017) found that using single dry gas viscosity and compressibility factor
162 effect the performance prediction of gas condensate reservoirs. Well known method of Lee-
163 Gonzalez-Eakin, (1966), which originally developed from natural dry gas, is used in most of
164 PVT software due to its simplicity. Londono et al., (2002) and Sutton, (2005) examined
165 applicability of the LGE correlation to predict gas viscosity in low to high gas specific
166 gravities. Londono et al., reported average absolute error of 3.34% and Sutton, (2005)
167 reported average absolute error of 22.6% for their entire database. Another study by Al-

168 Nasser and Al-Marhoun, (2012) shows that LGE predicts gas viscosity with maximum error
 169 of 16.81 within $0.55 < \gamma_g < 1.55$. Elsharkawy, (2006) also reported 13.8 average absolute
 170 error using LGE method over the range of $0.566 < \gamma_g < 1.895$. All aforementioned studies
 171 were confirming that LGE method is not suitable for modelling gas condensate viscosity
 172 below the dew point. Hence in this study an attempt was made to optimize the existing well
 173 known viscosity correlations, for better modelling of gas condensate reservoirs through
 174 establishing new Inflow Performance Relationship (IPR). For this purpose two sets of
 175 experimental data by Al-Meshari et al., (2007) and Yang et al., (2007) selected. These
 176 studies carried out in elevated pressure and temperature in laboratory condition similar to
 177 the reservoir temperature and pressure condition. The fluids used in these experimental
 178 studies are from gas condensate reservoirs in Saudi Arabia and North Sea. The collected
 179 fluids (gas and liquid) recombined in laboratory and viscosity measurement were made (Al-
 180 Meshari et al., 2007; Yang et al., 2007).

181 Prediction performance of Lee et al., 1966, (LGE) , Lohrenz et al., 1964, (LBC), Londono et
 182 al., (2002), Sutton, (2005) and Elsharkawy, (2006) are tested against the experimental data.
 183 These correlations are typically used for predicting viscosity in PVT software. Average
 184 Absolute Relative Deviation (AARD%) of each model performed using Eq. (1). The
 185 performance of each method is presented in Fig. 1.

$$AARD\% = \frac{1}{Np} \sum_{i=1}^N \left| \frac{\mu_i^{experiment} - \mu_i^{calculated}}{\mu_i^{experiment}} \right| \times 100 \quad (1)$$

186



187

188 **Fig. 1.** Average absolute relative deviation percentage (AARD %) of each method in predicting gas
 189 condensate viscosity.

190 The correlation proposed by Londono et al., (2002) provides best performance in predicting
 191 experimental viscosity data, hence it has been selected for further modification. Londono et
 192 al., (2002) used an extensive data bank (4909 data sets) to modify Lee-Gonzalez-Eakin,
 193 (1966) for predicting viscosity of hydrocarbon mixture. The original form of Londono et al,
 194 (2002) given in equation 2 to 5.

$$195 \quad \mu_g = 10^{-4} K \exp[X \rho_g^Y] \quad (2)$$

196 Where:

$$197 \quad K = \frac{(16.7175 + 0.0419188Mg)T^{1.40256}}{212.209 + 18.1349Mg + T} \quad (3)$$

$$198 \quad Y = 1.09809 - 0.0392581X \quad (4)$$

$$199 \quad X = 2.12575 + \frac{2063.71}{T} + 0.011926Mg \quad (5)$$

$$200 \quad \rho_g = 1.601846 \times 10^{-2} \frac{Mg \cdot P}{RT} \quad (6)$$

201 Where T is temperature in Rankine (°R), ρ_g is gas density in g/cc, P is pressure in psia; Mg
 202 is gas molecular weight and R is universal gas constant (10.732) psia cuft/[lb-mole-°R].

203 In an attempt to minimize the error between experimental data and the Londono correlation
 204 a non-linear regression model on MATLAB was used. Londono et al., (2002) model was cast
 205 in the following form:

$$206 \quad \mu_g = aK \exp\left[X \left(\frac{\rho_g}{b}\right)^Y\right] \quad (7)$$

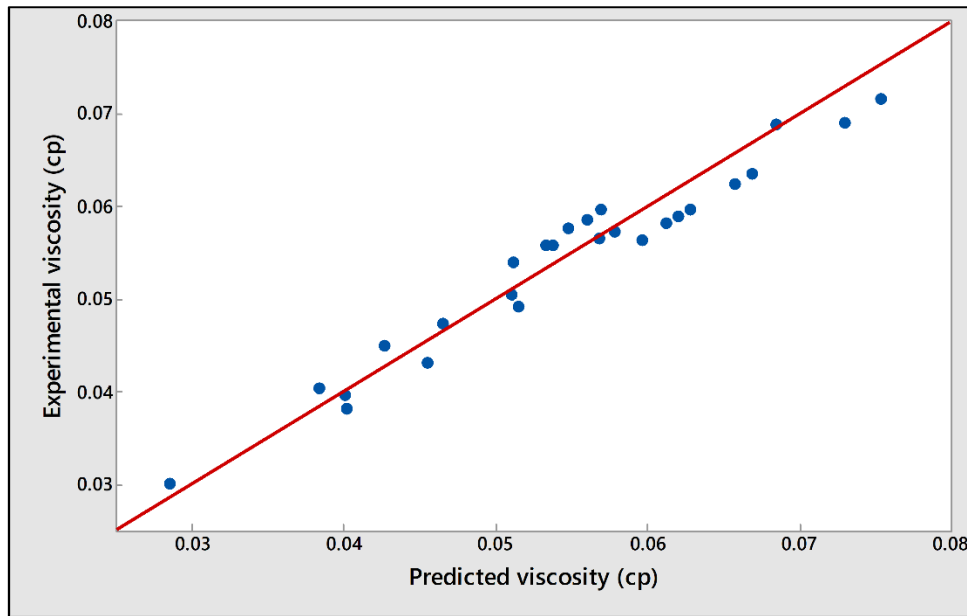
207 Where “a” and “b” are the optimized coefficient for the model as follow:

$$208 \quad \left\{ \begin{array}{l} a = 0.000246933 \\ b = 27.6718 \end{array} \right\}$$

209 As a result of this analysis new gas condensate viscosity model is proposed in Eq. (8).

$$210 \quad \mu_{gc} = 0.000246933K \exp\left[X \left(\frac{\rho_g}{27.6718}\right)^Y\right] \quad (8)$$

211 The parameters of K, Y and X are same as the original Lee et al., (1966) equation. 50% of
 212 the experimental data were used for developing regression model in Eq. (8). The remaining
 213 50% of the data used to test the performance of the model. The performance of the model
 214 plotted against the experimental data and shown in Fig. (2). New developed model is
 215 predicting experimental data with 5.2% AARD %. Eq. (8) will be used in modelling PVT
 216 properties of gas condensate reservoir later in this study.



217

218

Fig 2. Plot of calculated vs. the measured viscosity data.

219 Accurate prediction of gas condensate reservoirs require using more accurate
 220 compressibility factor (Elsharkawy et al., 2000; Whitson et al., 1999). In fact compressibility
 221 factor dictates gas and condensate recoveries in gas condensate reservoirs (Whitson et al.,
 222 2000, 1999). Studies by Behmanesh et al., (2017) Arukhe and Mason, (2012) elucidate that
 223 use of single phase compressibility factor underestimate the production in gas condensate
 224 reservoirs. Hence for better prediction of performance, two-phase compressibility factor
 225 correlation, developed by Rayes et al., (1992), shown in Eq. (9) utilized to model PVT. Their
 226 method is applicable to rich gas condensate reservoirs with pseudo-reduced pressure range
 227 of $0.7 \leq Pr \leq 20$ and temperature range of $1.1 \leq Tr \leq 2.1$.

$$228 \quad Z_{2p} = A_0 + A_1(P_{pr}) + A_2\left(\frac{1}{T_{pr}}\right) + A_3(P_{pr})^2 + A_4\left(\frac{1}{T_{pr}}\right)^2 + A_5\left(\frac{P_{pr}}{T_{pr}}\right) \quad (9)$$

229 Where $A_0 = 2.2435$, $A_1 = -0.03752$, $A_2 = -3.5653$, $A_3 = 0.0008292$, $A_4 = 1.5342$, and
 230 $A_5 = 0.131987$.

231 Accurate prediction of compressibility factor is function of accurate pseudo-critical properties
 232 of pressure (P_{pc}) and temperature (T_{pc}). To determine more accurate pseudocritical
 233 properties Eq. (10) and Eq. (11) proposed by Sutton, (2005) were also employed in this
 234 study. According to Sutton, (2005) these two equations outperform other well-known pseudo
 235 critical properties in the literature such as Elsharkawy et al., (2000), Sutton, (1985) and Piper
 236 et al.,(1993).

$$237 \quad P_{pc} = 744 - 125.4\gamma_g + 5.9\gamma_g^2$$

238 (10)

$$T_{pc} = 164.3 + 357.7\gamma_g - 67.7\gamma_g^2$$

(11)

241

242 New viscosity correlation Eq. (8), two-phase compressibility factor in Eq. (9) and pseudo-
 243 critical properties Eq. (10) and Eq. (11) are used to complete material balance calculation
 244 and generate gas phase PVT properties. An algorithm flowchart in Fig. 3 shows the
 245 calculation steps to complete PVT calculation.

246

247

248

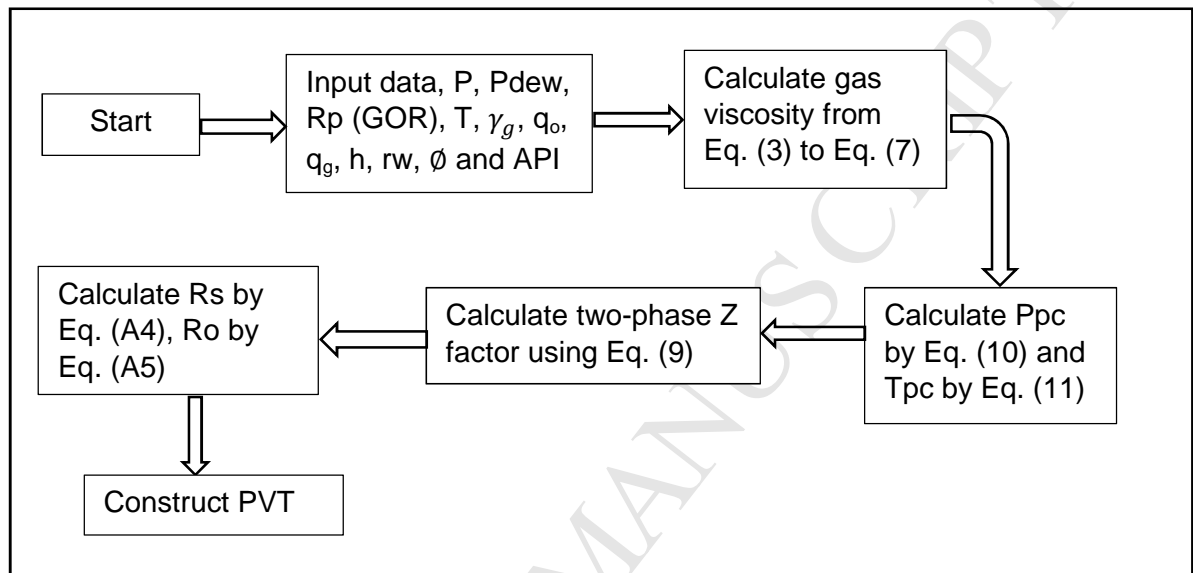
249

250

251

252

253



254

Fig. 3. Flow chart for computing PVT properties of gas phase.

255

256

257

258

259

260

261

262

263

There are many models in the literature for performance modelling of gas condensate through establishing Inflow Performance Relationship (IPR) curves. This include (Fevang and Whitson, 1996; Guehria, 2000; Jokhio et al., 2002; Jokhio and Tiab, 2002; Mott, 2003; Qasem et al., 2014; Shahamat et al., 2015; Sousa et al., 2017). However, PVT calculation in aforementioned methods completed with the assumption of single phase flow. In Jokhio and Tiab, (2002) single phase correlations were applied to model PVT, then tabulated PVT used in calculating of pseudopressure integrals. In this study the performance of high temperature heavy gas condensate reservoir is determined by implementation of two new gas condensate viscosity and two phase compressibility factor.

264

3. Two phase pseudopressure approach

265

266

267

268

Pseudopressure approach is a simple and convenient method of handling the nonlinearity in gas condensate reservoirs and establishing IPR (Bonyadi et al., 2012; Fevang and Whitson, 1996; Kniazeff and Naville, 1965; Mott, 2003). The fundamental gas flow rate equation is proposed by Rawlins and Schellhardt, (1936), shown in Eq. (12) This back pressure

269 equation, which developed as a results of several hundred wells studies is relating gas rate
270 to bottom-hole flowing pressure (P_{wf}).

$$271 \quad q_{gt} = C(P_{avg}^2 - P_{wf}^2)^n \quad (12)$$

272 In terms of pseudopressure Eq. (12) can be written as follow:

$$273 \quad q_{gt} = C_g(\Delta m P_{gt})^n \quad (13)$$

274 Where C is productivity index, $\Delta m P_{gt}$ is total gas pseudopressure function, n is exponent and
275 q_{gt} is total gas flow rate. Productivity index C depends on well and reservoir geometry, that
276 can be estimated mathematically from Eq. (14) for gas phase and Eq. (15) for oil phase.
277 During pressure build up test the values of gas and condensate flow rates are measured at
278 the surface. Semi log-log plot of pseudopressure $\Delta m P$ against measured flow rates form a
279 straight line. The intercept of this straight line is the value of C and the slope is n (Ahmed,
280 2010; Guo et al., 2008; Roussennac, 2001; Stewart, 2011). In this study similar concept has
281 been applied, utilizing pressure test data to determine productivity index and coefficient n.

$$282 \quad C_g = \frac{0.00708.kh}{\ln\left(\frac{r_e}{r_w}\right) - 0.75 + s} \quad (14)$$

$$283 \quad C_o = \frac{0.00708.kh}{\ln\left(\frac{r_e}{r_w}\right) - 0.75 + s} \quad (15)$$

284 The constant C includes basic reservoir properties such as permeability, thickness h,
285 drainage radius, r_e ; well bore radius, r_w ; skin factor, s; and other constants (Bonyadi and
286 Rostami, 2017; Jokhio and Tiab, 2002; Lyons et al., 2016; Mott, 2003).

287 $\Delta m P_{gt}$ in Eq. (13) is a two-phase pseudopressure function that can be calculated from two
288 phase pseudopressure integral proposed by Fevang and Whitson, (1996). Their integral in
289 terms of effective permeability ($k \cdot k_{rg}$) is shown in Eq. (16).

$$\Delta m P_{gt} = \left\{ \int_{P_{dew}}^{P_{avg}} \left(\frac{k \cdot k_{rg}(S_{wi})}{B_{gd}\mu_g} \right) dp + \int_{P^*}^{P_{dew}} \left(\frac{k \cdot k_{rg}}{B_{gd}\mu_g} \right) dp + \int_{P_{wf}}^{P^*} \left(\frac{k \cdot k_{rg}}{B_{gd}\mu_g} + \frac{k \cdot k_{ro}}{B_c\mu_o} R_s \right) dp \right\} \quad (16)$$

290 Where: P_{avg} is average reservoir pressure, P_{dew} is dew point pressure, S_{wi} is the initial water
291 saturation, k is absolute permeability, kr: phase relative permeability, P^* is the pressure in
292 the interface between Region 1 and Region 2, P_{wf} is bottom hole flowing pressure, Bgd is
293 dry gas formation volume factor, Bo is oil formation volume factor, μ is viscosity and R_s is
294 solution gas to oil ratio (GOR).

295 In Eq. (16) the first integral, with integral limits P_{dew} to P_{avg} , relates to Region 3, in which
296 only gas phase is present. The second integral, with the integral limits P^* to P_{dew} , relates to

297 Region 2, in which condensate drop-out, but its saturation is less than critical condensate
 298 saturation. Hence, it is immobile and only the gas phase is flowing. The third integral, with
 299 the integral limits P_{wf} to P^* , relates to Region 1, near wellbore region, in which both gas and
 300 condensate phases are flowing simultaneously at different velocities. The flow in this region
 301 is steady state flow, meaning what comes into Region 1 through its outer boundary, will flow
 302 at and will be produced at the surface with no net accumulation of fluid. Region 1 is the main
 303 source of deliverability loss due to condensate build up, which decreases relative
 304 permeability to gas in gas condensate reservoirs (Behmanesh et al., 2017; Bonyadi et al.,
 305 2012; Bonyadi and Rostami, 2017; Fevang and Whitson, 1996; Hekmatzadeh and Gerami,
 306 2018; Mott, 2003; O'Dell and Miller, 1967).

307 Existence of the aforementioned regions in gas condensate reservoirs is a function of
 308 pressure. If bottom-hole flowing pressure is less than the dew point pressure ($P_{wf} < P_{dew}$),
 309 Region 1 will always exist; and if bottom hole flowing pressure is higher than the dew point
 310 pressure ($P_{wf} > P_{dew}$), Region 1 will not exist (Fevang and Whitson, 1996; Wheaton and
 311 Zhang, 2007). If pressure interface between Region 1 and 2 (P^*) is bigger than average
 312 reservoir pressure [$P^* > P_{avg}$], then integration of Region 1 pressure function should be only
 313 from P_{wf} to P_{avg} . In this case Region 2 and 3 don't exist (Fevang, 1995; Fevang and
 314 Whitson, 1996), then the first two integral terms can be ignored in the calculation. This is
 315 happening in highly saturated gas condensate reservoirs (Fevang, 1995; Fevang and
 316 Whitson, 1996; Jokhio and Tiab, 2002). In this case ($P^* > P_{avg}$), only third part of the
 317 pseudopressure integral in Eq. (16), which devoted for Region 1, is used with pressure limits
 318 from P_{wf} to P_{avg} .

319 Similar concept is used in this study and Eq. (17) has been used to calculate
 320 pseudopressure function. This is because the well that was selected for this study is
 321 producing heavy condensate and is very high in temperature (Economides et al., 1989).
 322 Region 2 and 3 did not develop in such reservoirs and condensation start from the beginning
 323 of the production.

$$\Delta m P_{gt} = \int_{P_{wf}}^{P_{avg}} \left(\frac{k \cdot k_{rg}}{B_{gd} \mu_g} + \frac{k \cdot k_{ro}}{B_o \mu_o} R_s \right) dp \quad (17)$$

324 The PVT properties, producing gas/oil ratio (GOR) R_p and gas/oil effective permeabilities
 325 are needed to evaluate pseudopressure integral in Eq. (17) (Bonyadi et al., 2012; Fevang
 326 and Whitson, 1996; Guehria, 2000; Mott, 2003). P_{wf} and P_{avg} , are known based on well
 327 pressure build up test.

328 Producing gas to oil ratio, R_p is a ratio of total gas production to total oil production on the
 329 surface. Eq. (18) (Ahmed, 2010; Fetkovich et al., 1986; Fevang and Whitson, 1996;
 330 Guehria, 2000; Jokhio and Tiab, 2002).

$$R_p = \frac{q_{gt}}{q_{ot}} = \frac{C_g \left[\left(\frac{k_{rg}}{B_{gd}\mu_g} \right) + \left(\frac{k_{ro}}{B_o\mu_o} \right) R_s \right]}{C_o \left[\left(\frac{k_{rg}}{B_{gd}\mu_g} \right) R_o + \left(\frac{k_{ro}}{B_o\mu_o} \right) \right]} \quad (18)$$

331 Where, R_o is oil to gas ratio (STB/scf), q_{gt} and q_{ot} are total gas flow rate and total oil flow
 332 rate respectively. On simplification of Eq. (18), R_p can be presented in Eq. (19) (Fetkovich et
 333 al., 1986; Fevang, 1995).

$$R_p = R_s + \left(\frac{k_{rg}}{k_{ro}} \right) \left(\frac{B_o\mu_o}{B_{gd}\mu_g} \right) (1 - R_o R_p) \quad (19)$$

334 Fetkovich et al., (1986), rearranged and solved Eq. (19) for k_{rg}/k_{ro} as it is shown in Eq. (20).
 335 This expression gives the ratio of (k_{rg}/k_{ro}) as a function of pressure.

$$\frac{k_{rg}}{k_{ro}}(P) = \frac{(R_p - R_s)}{(1 - R_o R_p)} \left(\frac{B_{gd}\mu_g}{B_o\mu_o} \right) \quad (20)$$

336 One of the primary objectives of this study was to determine effective permeabilities of gas
 337 and oil using well pressure test data. Hence, Evinger and Muskat, (1942), which indicates
 338 relative permeabilities K_{rg} and K_{ro} can be expressed directly as a function of ratio ($K_{rg}/$
 339 K_{ro}), when both phases are mobile, is used. Therefore Eq. (20) in terms of effective
 340 permeability rewritten and yields Eq. (21) for gas phase and Eq. (22) for oil phase. These
 341 two equations are showing that the effective permeability of one phase can be calculated
 342 from the other phase.

$$k_{eg} = k k_{rg} = \frac{(R_p - R_s)}{(1 - R_o R_p)} \left(\frac{B_{gd}\mu_g \{k k_{ro}\}}{B_o\mu_o} \right) \quad (21)$$

$$k_{eo} = k k_{ro} = \frac{(1 - R_o R_p)}{(R_p - R_s)} \left(\frac{B_o\mu_o \{k k_{rg}\}}{B_{gd}\mu_g} \right) \quad (22)$$

343 Where, k_{eg} and k_{eo} are gas and oil effective permeabilities respectively. Substituting Eq.
 344 (21) in Eq. (16) and simplifying yields gas pseudopressure integral in terms of effective
 345 permeability (Fetkovich et al., 1986; Fevang and Whitson, 1996; Guehria, 2000).

$$\Delta m P_{gt} = \int_{p_{wf}}^{P_{avg}} \left(\frac{k \cdot k_{rg}}{B_{gd}\mu_g} \right) \frac{R_p (1 - R_o R_s)}{(R_p - R_s)} (P) dp$$

346 Pseudopressure integrals in Eq. (23) can be computed through the reformulation by Jokhio
 347 and Tiab, (2002) in Eq. (24).

$$\Delta m P_{gt} = \left[\int_{p_{wf}}^{P_{avg}} \left(\frac{1}{B_{gd} \mu_g} \right) \frac{R_p (1 - R_o R_s)}{(R_p - R_s)} (P) dp \right] \times \int_{p_{wf}}^{P_{avg}} k \cdot k_{rg}(P) dp \quad (24)$$

348 Based on conventional assumption of transient fluid flow and fluid superposition principle,
 349 the pseudopressure integral can be obtained as shown in Eq. (25) (Earlougher, 1977;
 350 Horner, 1951; Serra et al., 2007; Stewart, 2012).

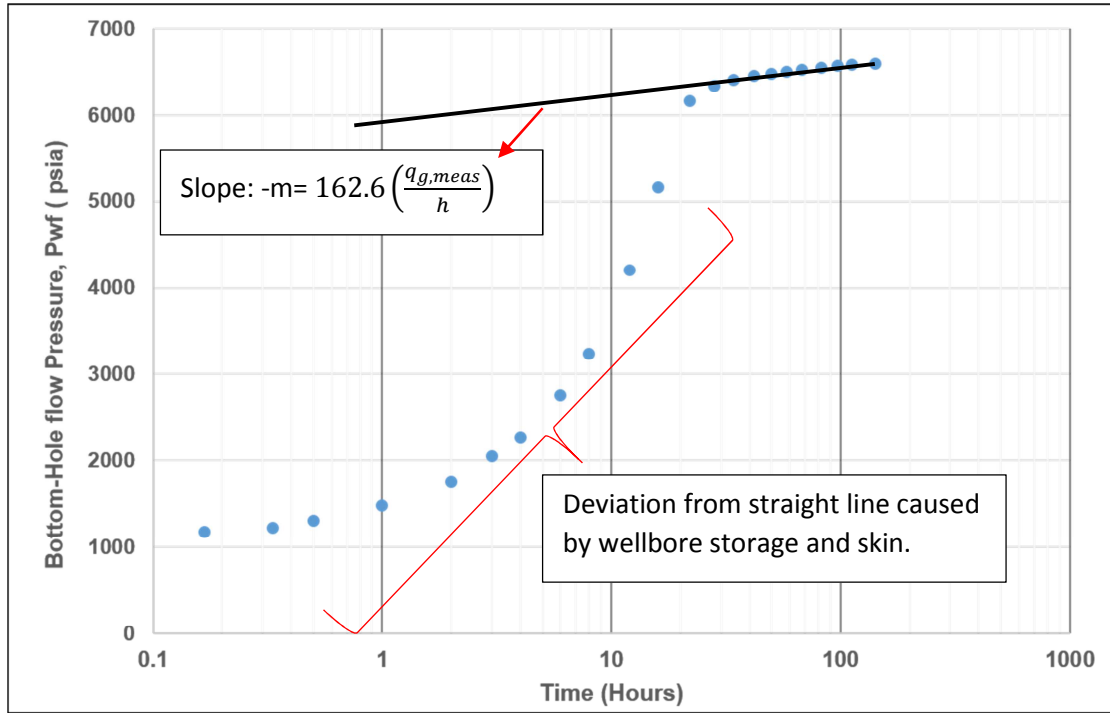
$$\int_{p_{wf}}^{P_{avg}} \left(\frac{k \cdot k_{rg}}{B_{gd} \mu_g} \right) \frac{R_p (1 - R_o R_s)}{(R_p - R_s)} (P) dp \quad (25)$$

$$= 162.6 \left(\frac{q_{g,meas}}{h} \right) \left(\log(t) + \log \left(\frac{keg(p)}{\phi \mu_g c_t r_w^2} \right) - 3.23 + 0.87s \right)$$

$$\int_{p_{wf}}^{P_{avg}} k \cdot k_{rg}(P) dp = 162.6 \frac{q_{g,meas}}{h \left(\frac{d\Delta m P_g}{d \ln(t)} \right)} \quad (26)$$

351 This allows the integral in Eq. (24) to be solved without the need of relative permeability
 352 curve, which is plotted as a function of saturation.

353 In Eq. (25), $q_{g,meas}$ is measured gas flow rate at surface during the test; t is recorded
 354 pressure test time; h is reservoir thickness; keg is effective permeability of gas phase; ϕ is
 355 porosity of the media; μ_g is gas viscosity; c_t is total compressibility factor; r_w is wellbore
 356 radius; and s is skin factor. Right hand side of Eq. (25) is pressure build up equation
 357 originally proposed by Horner, (1951) and modified by Earlougher, (1977). This equation is
 358 based on conventional assumption of transient fluid flow and superposition principles. The
 359 assumption indicates semi log plot of recorded time against well flow bottom-hole pressure
 360 (P_{wf}), provides straight line with a slope of $162.6 \left(\frac{q_{g,meas}}{h} \right)$ and intercept of $\left[\log(t) + \right.$
 361 $\left. \log \left(\frac{keg(p)}{\phi \mu_g c_t r_w^2} \right) - 3.23 + 0.87s \right]$ (Ahmed, 2010; Dake, 2001; Earlougher, 1977; Roussennac,
 362 2001; Serra et al., 1990). Fig. 4 shows this relation graphically where recorded time of the
 363 pressure build up test is plotted against (P_{wf}) in a heavy gas condensate well (KAL05). The
 364 plot in Fig 4 commonly referred as Horner plot. An early time deviation from the graph can
 365 be caused by wellbore storage effect and skin factor (Ahmed, 2010; Roussennac, 2001).
 366 This deviation is large if permeability is low and compressibility is high. This is the case in
 367 heavy gas condensate reservoir, where the liquid evolves from the gas in early stages, as it
 368 shown in Fig. (4).



369

370

Fig. 4. Horner plot for KAL-5 gas condensate well (data after Economides, 1989).

371 Gas phase effective permeability integral as a function of pressure can be estimated by Eq.
 372 (26) (Jokhio et al., 2002), where $d\Delta mPg/d\ln(t)$ is the derivative function of gas phase. Eq.
 373 (26) specifies that the effective permeability integral is inversely proportional to the derivative
 374 of the pressure with natural logarithmic of time. On semi log plot of time against
 375 pseudopressure, the rate of change of pseudopressure is the slope of a straight line (Jokhio
 376 and Tiab, 2002; Serra et al., 2007). This will provide an equation for straight portion of the
 377 graph in Fig. 4. To evaluate effective permeability integral in Eq. (26), pseudopressure
 378 derivative group $d\Delta mPg/d\ln(t)$ is needed, which can be estimated using Eq. (27) after
 379 Jokhio and Tiab, (2002).

$$\left(\frac{d\Delta mP}{d\ln(t)} \right)_i = \frac{\left(\frac{d\Delta mP_{i-1}}{d\ln(t)_{i-1}} \right) \Delta \ln(t)_{i+1} + \left(\frac{d\Delta mP_{i+1}}{d\ln(t)_{i+1}} \right) \Delta \ln(t)_{i-1}}{[\Delta \ln(t)_{i+1} + \Delta \ln(t)_{i-1}]} \quad (27)$$

380 Where, the point i is the point, where the derivative is calculated and point $(i - 1)$ is the point
 381 before it and $(i + 1)$ is the point after it. Pseudopressure difference is calculated from
 382 $(\Delta mP = mP - mP_{(t=0)})$, which is the difference in pseudopressure of any given pressure and
 383 pseudopressure at the beginning of the pressure build up test.

384 For condensate (oil) phase the two-phase pseudopressure function can be written as Eq.
 385 (28) (Fevang, 1995, 1995; Jokhio et al., 2002; Penula, 2003). Substituting Eq. (21) and Eq.
 386 (22) in Eq. (28) and simplifying yields Eq. (29), which represents condensate (oil) phase

387 pseudopressure function in terms of effective permeability (Fetkovich et al., 1986; Fevang
388 and Whitson, 1996; Guehria, 2000; Penula, 2003)

$$\Delta mP_{ot} = \int_{P_{wof}}^{P_{avg}} \left(\frac{k \cdot k_{ro}}{B_o \mu_o} + \frac{k \cdot k_{rg}}{B_g \mu_g} R_o \right) dp \quad (28)$$

$$\Delta mP_{ot} = \left[\int_{p_{wof}}^{P_{avg}} \left(\frac{K \cdot Kr_o}{B_o \mu_o} \right) \frac{(1 - R_o R_s)}{(1 - R_o R_p)} (P) dp \right] \quad (29)$$

389 Jokhio and Tiab, (2002) reformulate and present the oil phase pseudopressure integral in
390 form of Eq. (30), using generalized superposition equation to model the effective
391 permeability directly by well pressure build up data. Oil phase effective permeability integral
392 can be calculated using Eq. (31).

$$\Delta mP_{ot} = \left[\int_{p_{wof}}^{P_{avg}} \left(\frac{1}{B_o \mu_o} \right) \frac{(1 - R_o R_s)}{(1 - R_o R_p)} (P) dp \right] \times \int_{P_{wof}}^{P_{avg}} k \cdot k_{ro}(P) dp \quad (30)$$

$$\int_{P_{wof}}^{P_{avg}} k \cdot k_{ro}(P) dp = 162.6 \frac{q_{o,meas}}{h \left(\frac{d\Delta mP_o}{d\ln(t)} \right)} \quad (31)$$

393 Pseudopressure and its derivative $(d\Delta mP_o)/d\ln(t)$ in Eq. (31) can be computed using Eq.
394 (27). Similar to gas phase back pressure equation of Rawlins and Schellhardt, (1936), Eq.
395 (32) can be used to estimate the total oil flow rate.

$$396 \quad q_{ot} = C_o (\Delta mP_{ot})^n \quad (32)$$

397 Having calculated pseudopressure function in any given pressure logarithmic plot of mP
398 against measured flow rates (gas, oil) at the surface, provides a straight line. The slope of
399 this straight line is coefficient 'n' and intercept is 'C' in Eq. (13) and Eq. (32) for gas and oil
400 phase respectively. Hence gas flow rate in each pressure step can be calculated using Eq.
401 (13); and Inflow Performance Relationship (IPR) curve can be established. To determine
402 condensate phase IPR similar procedure were also used.

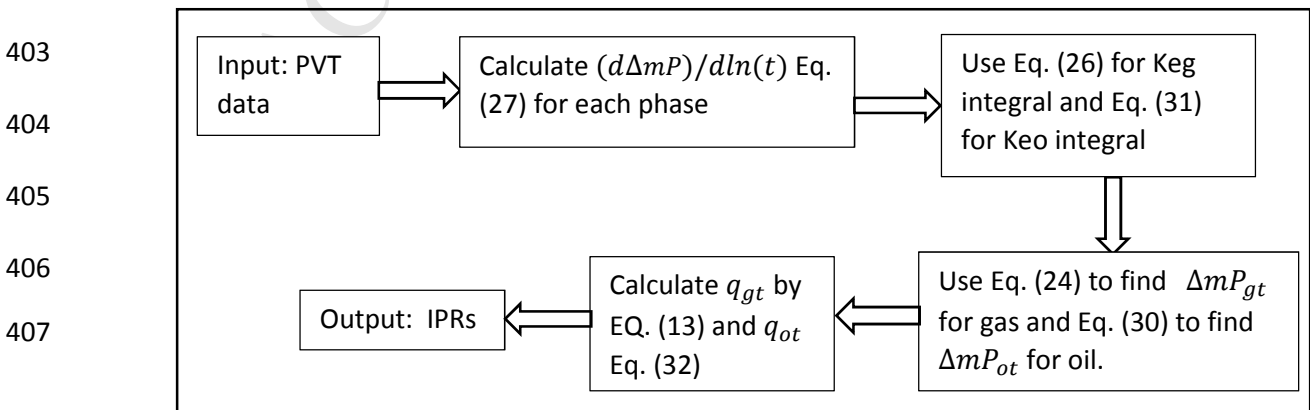


Fig. 5. Flowchart for computing pseudopressure integrals and construct IPRs.

408 3.1 Methodology to use the new IPR model

409 To establish gas phase IPR, for given bottom-hole flowing pressure (P_{wf}), the calculation
410 procedure can be summarized as follow:

- 411 1. Calculate PVT properties for gas phase, using new viscosity correlation Eq. (7) and
412 two-phase compressibility factor Eq. (9). Detail calculation of PVT are provided in
413 Appendix A for gas phase and Appendix C for condensate phase.
- 414 2. Calculate pseudopressure derivative group $(d\Delta mP)/d\ln(t)$ using Eq. (27) for each
415 phase. Use recorded time (t) and bottom-hole flowing pressure (P_{wf}) from pressure
416 build up test data.
- 417 3. Calculate effective permeability integral for any given pressure using Eq. (26) for gas
418 phase and use Eq. (31) for condensate phase.
- 419 4. Calculate pseudopressure function using Eq. (24) for gas phase and Eq. (30) for
420 condensate phase. Evaluate the integral by trapezoidal rule of integration. A sample
421 of numerical evaluation of pseudopressure integral is presented in Appendix B.
- 422 5. Evaluate productivity index (C) and coefficient (n) using plot of pseudopressure
423 function against flow rate on a log-log scale to form a straight line. Slope of this
424 straight line is n and intercept is C . Gas and condensate flow rates can be obtained
425 from pressure build up test.
- 426 6. Having calculated C and n for gas and condensate phase evaluate gas flow rate by
427 Eq. (13) and condensate flow rate by Eq. (32).
- 428 7. Plot the bottom-hole flow pressure (P_{wf}) against the flow rates to establish Inflow
429 Performance Relationship (IPR) curve.

430 4. Validation of New IPR model

431 The validity of the new IPR model is verified by compositional simulation of a high
432 temperature rich gas condensate well, using Schlumberger (PIPSIM) simulator. Results of
433 transient pressure test data is obtained from Economides et al., (1989) and used to validate
434 the developed IPR model. This vertical well named (KAL-5) located in a Permian basin in a
435 very high temperature formation (365 °F at 11,500 ft [180°C at 3500m]), which produces gas
436 and heavy condensate. The physical properties of the reservoir and well is presented in
437 Table 1. Reservoir and well geometry is obtained from Economides et al., (1989) and Jokhio
438 and Tiab, (2002). The flow rate during the well test was 75.4 Mscf/day [2135 std m³/day] of
439 gas and 2.8 STB/day [0.45 m³/day] of condensate. API gravity is assumed to be 50 to match
440 the gas condensate gravity which is typically in the range of 40 to 60 API (McCain and
441 Cawley, 1991; Whitson et al., 2000). Table 2 includes fluid molar composition of the
442 reservoir (Economides et al., 1989). During the test, well flowed for 103 hours and then was

443 subjected to 141 hours pressure buildup. The initial reservoir pressure is 6750psia and it is
 444 almost identical to retrograde condensation point. Condensation of the gas started from the
 445 beginning of the production and entire reservoir is in two-phase flow condition. This condition
 446 is same as near well-bore region, Region 1, where combination of oil and gas are
 447 simultaneously flow.

448 **Table 1**

449 Well and reservoir data (Economides, et al., 1989).

| | | | |
|----------------------|--|------------|--|
| P _{initial} | 6750 psia | q_o | 2.8 STB/day = 0.45m ³ /day |
| P _{dew} | 6750 psia | H | 216.5ft = 65.98m |
| GOR | 9470 scf/STB=1686.67 m ³ /m ³ | ϕ | 0.062 |
| T | 356°F=180°C | r_w | 0.54ft = 0.16459m |
| Gas γ_g | 0.94 [MW=27.17] | API | 50 [Assumed] |
| q_g | 75.4 Mscf/day=2135 m ³ /day | ΔT | 2.85 °F/100FT |

450

451 **Table 2**

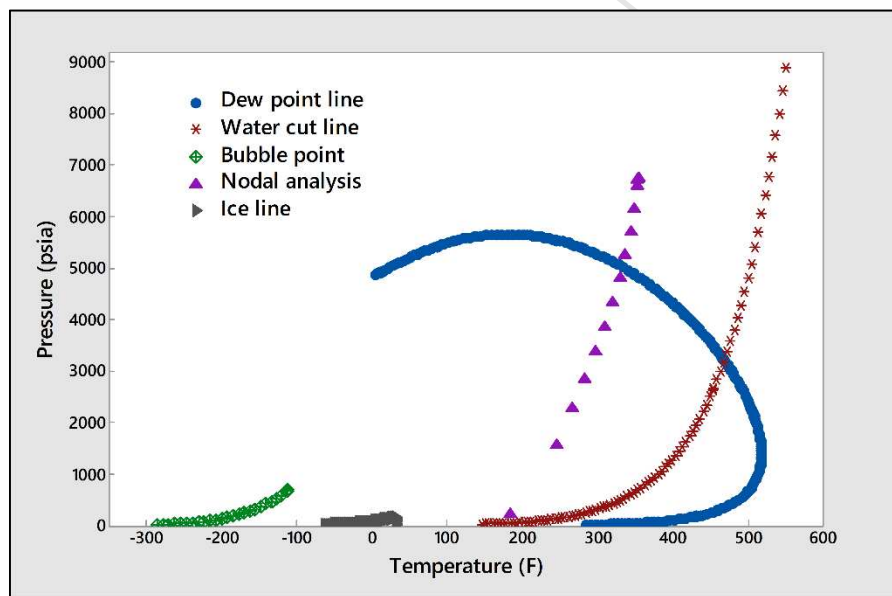
452 Reservoir Fluid molar composition information for well KAL-5.

| Components | % mole fraction |
|------------------|-----------------|
| H ₂ S | 0.006 |
| N ₂ | 1.452 |
| CO ₂ | 10.931 |
| C ₁ | 72.613 |
| C ₂ | 6.24 |
| C ₃ | 1.63 |
| i-C ₄ | 0.553 |
| n-C ₄ | 0.693 |
| i-C ₅ | 0.442 |
| n-C ₅ | 0.379 |
| C ₆ | 0.516 |
| C ₇ | 0.644 |
| C ₈ | 0.541 |
| C ₉ | 0.388 |
| C ₁₀₊ | 2.979 |

453

454 Multi flash compositional simulation of the condensate fluid performed on PIPSIM simulator.
 455 A vertical well is created using physical properties of the well shown in Table 1 and fluid
 456 properties in Table 2.

457 Fig. 6 shows the phase diagram of the heavy gas condensate well as a results of multi flash
 458 compositional simulation of the fluid sample in a standard condition (temperature of 60°F
 459 and pressure of 14.696psia). The dew point line in phase diagram indicates that the initial
 460 conditions coincide with the retrograde condensation, hence condensation begins from the
 461 begging of the production. This highlights the fact that using single phase correlation to
 462 model this type of reservoir fluid is oversimplify the modelling. As pressure declines to
 463 around 3000psia the water phase enters the hydrocarbon region and fluid become three
 464 phase (gas, condensate and water). Water cut of 30% is used in PVT calculation of the fluid.
 465 Three parameters Peng-Robinson, (1976) equation of state was used to complete the PVT
 466 calculation in the simulation study. Calculation include gas viscosity (μ_g), compressibility
 467 factor (Z), gas formation volume factor (Bg) and solution gas to oil ratio (Rs).



468
 469 **Fig. 6.** Pressure-Temperature diagram for KAL-5 gas condensate well.

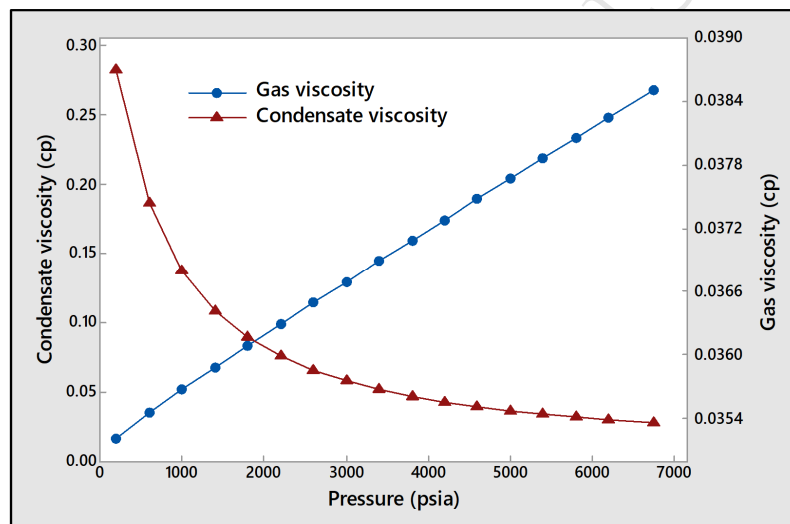
470 5. Results and discussion

471 Fig. 7 shows the variation of gas and condensate viscosity as a function of pressure for very
 472 high temperature rich gas condensate well (KAL-5). New gas viscosity correlation proposed
 473 by this study presented in Eq. (8), used to predict gas phase viscosity. Fig. 8 shows the
 474 different in gas viscosity using new gas viscosity correlation and LGE, (1964) correlation.
 475 New viscosity correlation provides gas condensate viscosity in lower range in compare to the
 476 LGE method. The experimental gas condensate viscosity data is used in developing new
 477 correlation to predict the gas viscosity in high temperature condition. The range of gas

478 viscosity is in agreement with the study of gas viscosity in high temperature and high
 479 pressure reservoirs by Davani et al., (2013) and Ling et al., (2009). They show that in the
 480 pressure range of $2000 < P < 7000 \text{ psia}$ and temperature range of $104 < T < 212^\circ\text{C}$
 481 variation in gas viscosity is very low. These studies also confirming increasing temperature
 482 and pressure in the reservoirs, result in decreasing the viscosity.

483 Explain more Graphical representation of compressibility factor as a function of pseudo
 484 reduced pressure presented in Fig 9. The two phase compressibility factor accounts for
 485 formation of liquid in reservoir formation. The result confirms using single phase
 486 compressibility factor for predicting two-phase system, underestimate productivity. As the
 487 pressure declines due to the production, single phase z-factor provide lower range of gas
 488 compressibility factor, whereas two phase compressibility factor predicts Z factor with a
 489 linear relationship to the pseudo-reduced pressure.

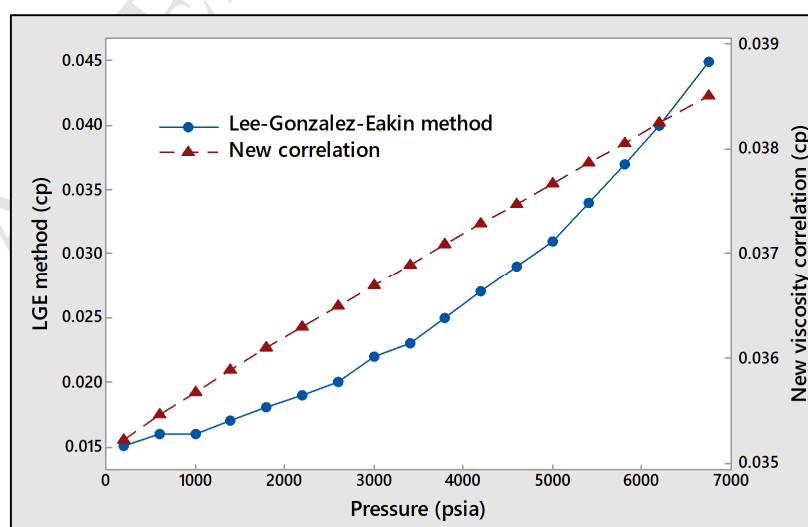
490



491

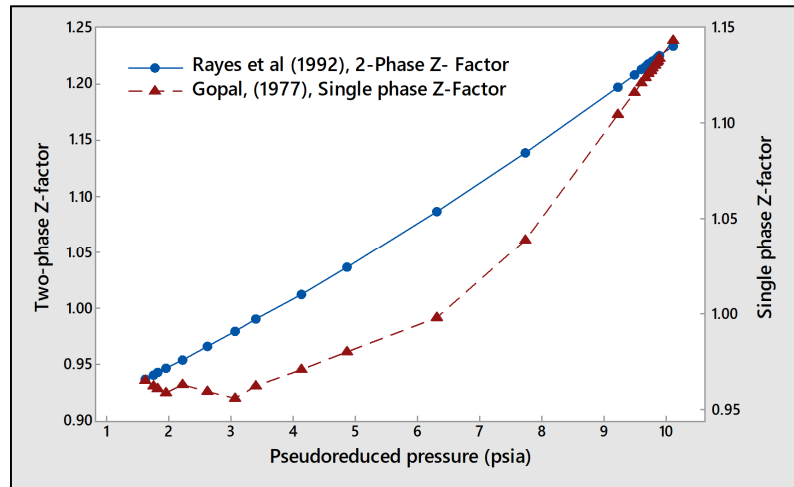
492

Fig. 7. Variation of gas and condensate viscosity with pressure.



493

494 **Fig. 8.** Comparison of gas phase viscosity using new developed correlation and LGE (1964)
 495 correlation.

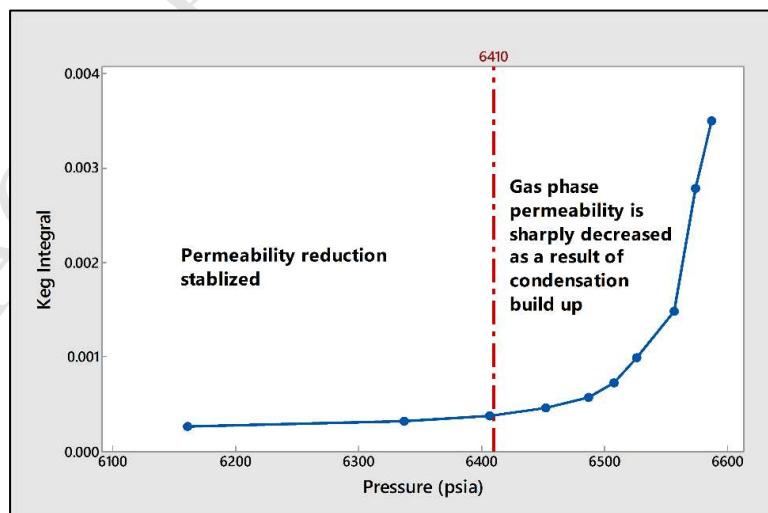


496

497

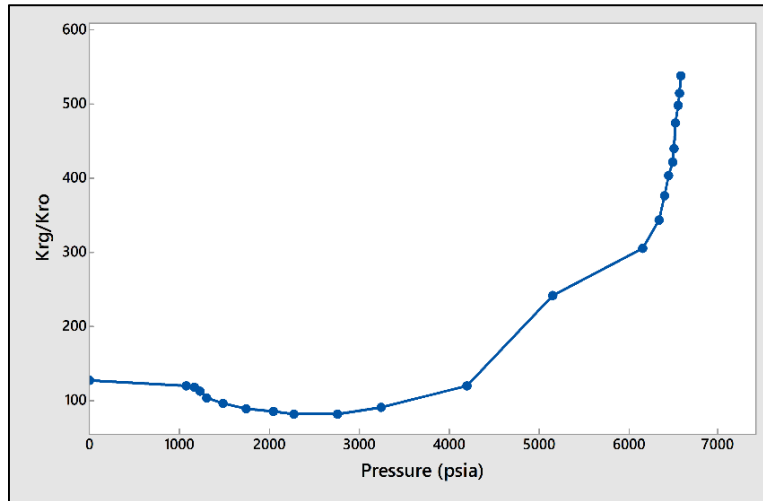
Fig. 9. Plot of z-factor vs pseudo reduced pressure.

498 Gas and condensate effective permeability integral is calculated using pseudopressure
 499 derivative function. The detail description of the calculation is given in Appendix B. The
 500 results of effective permeability integrals are illustrated in Fig. 10. The graph in Fig. 10
 501 shows that the effective permeability is dropped sharply when pressure declined, due to the
 502 condensate drop out and increasing liquid saturation. The results of effective permeabilities
 503 reconfirm the finding of Behmanesh et al., (2017); Fevang, (1995); Fevang and Whitson,
 504 (1996) and Mott, (2003), such that condensate drop out in gas condensate reservoirs leads
 505 to reduction in gas effective permeabilities. Relative permeability ratio of gas to oil (k_{rg}/k_{ro})
 506 also determined using Eq. (20) and presented in Fig. 11. The graph shows that the
 507 condensation build up, which starts in early stage of production leads to significant reduction
 508 in relative permeability to gas.



509
 510

Fig. 10. Gas phase effective permeability integrals.



511

512

Fig. 11. Relative permeability ratio (gas to oil) as a function of pressure.

513

514

515

516

517

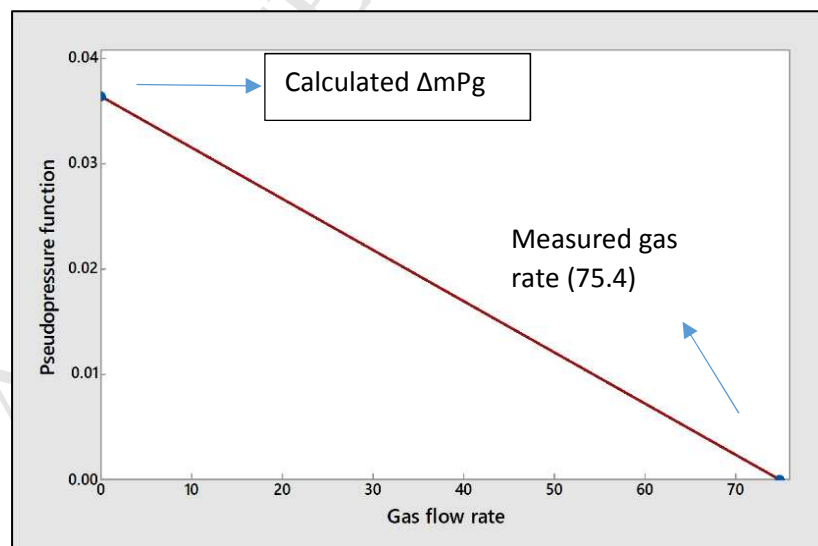
518

519

520

During well pressure build up test gas flow rate (q_g) and oil flow rate (q_o) were measured as previously shown in Table 1. Having calculated pseudopressure function ΔmP , allow to build a plot of flow rate against ΔmP . Fig. 12 shows the log-log plot of ΔmPg against gas flow rate, the intercept of the graph is productivity index C and gradient of the graph is value of coefficient n, in Eq. (13). Once these two aforementioned values are determined from the graph, Eq. (13), is applied to determine the gas rate for various bottom-hole flowing pressure (P_{wf}). Plotting the gas flow rate against P_{wf} establish the gas phase IPR, shown in Fig. (13). Condensate IPR is also established and presented in Fig. (14).

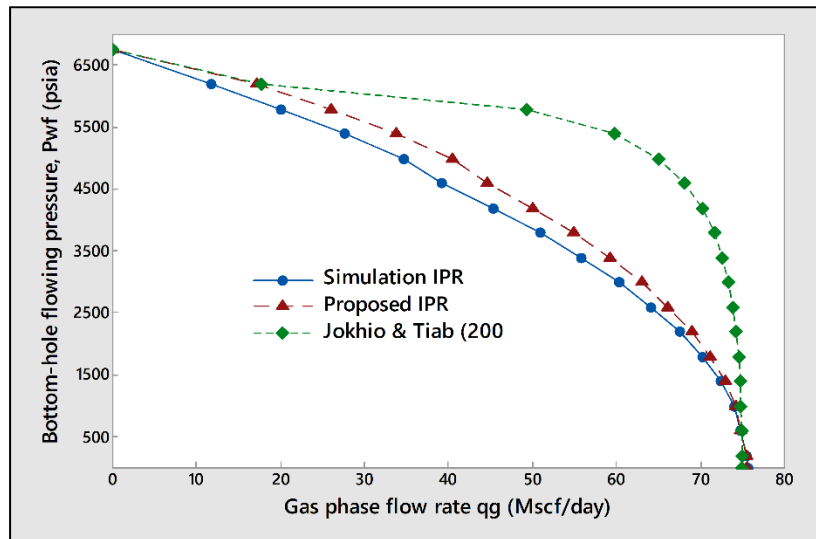
521



522

523

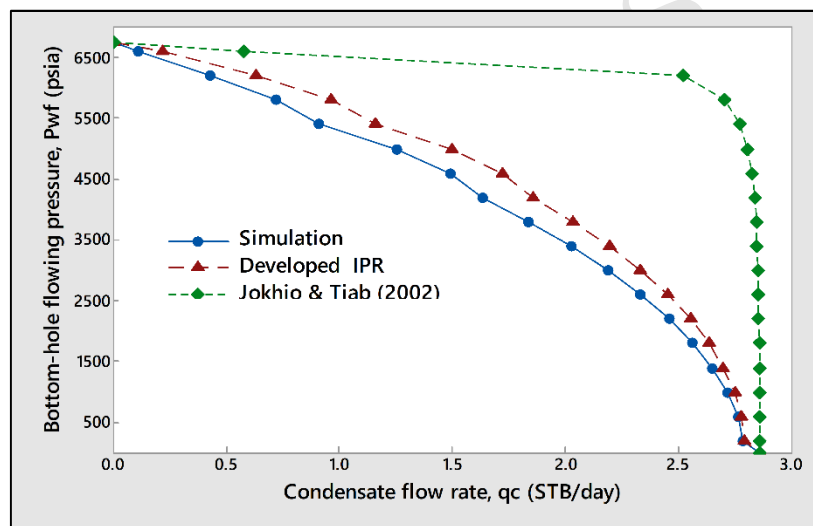
Fig. 12. Plot of gas flow rate against pseudopressure. [$n=0.8$] and $C=0.0948$].



524

525

Fig. 13. Gas phase IPR.



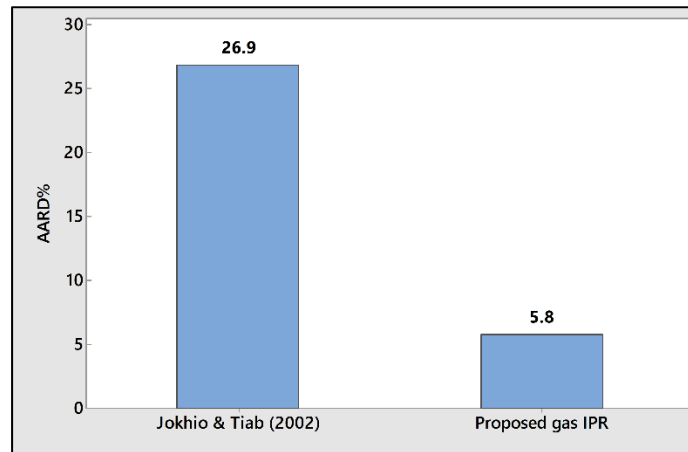
526

527

Fig. 14. Condensate phase IPR.

528 The average absolute relative deviation percent (AARD%) between the new developed IPR,
 529 Jokhio and Tiab, (2002) and simulation study of the well are estimated. The results of this
 530 error analysis is shown in Fig. (15) for gas phase and Fig. (16) for condensate phase. It is
 531 clear from the results that the new developed IPRs are in better agreement with simulation
 532 study with lower AARD%.

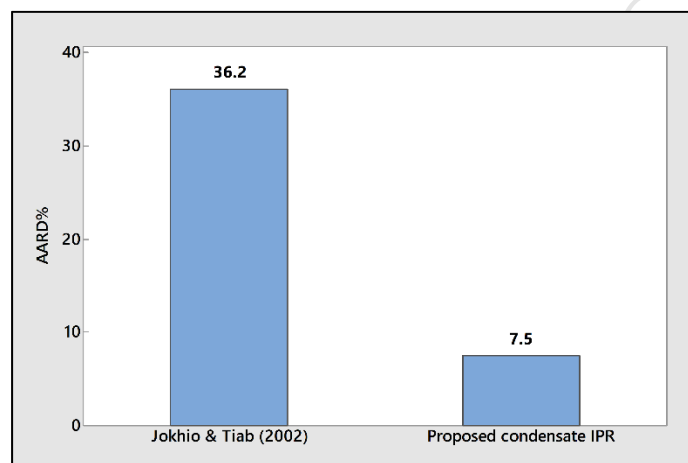
533



534

535

Fig. 15. The average absolute error deviation percent for gas phase IPR.



536

537

Fig. 16. The average absolute error deviation percent for condensate phase IPR.

538 The results of this study show that performance of high temperature heavy gas condensate
 539 well is a strong function of PVT properties include viscosity and compressibility. The
 540 characteristics of two-phase flow in gas condensate reservoirs are significantly different from
 541 conventional gas system. Single dry gas correlations cannot represent multiphase fluid
 542 behaviour of gas condensate reservoirs below the dew point.

543 6. Conclusions

544 In this study we generate IPR curves to predict the performance of depleting high
 545 temperature heavy gas condensate well. New developed gas condensate viscosity
 546 correlation and tow-phase compressibility factor is used in PVT calculation of
 547 pseudopressure function. The new IPR is compared to Jokhio and Tiab, (2002) and
 548 validated via compositional simulation study. Based on this work, the following can be
 549 concluded:

- 550 (1) A general correlation for viscosity " μ " of high temperature heavy gas condensate
 551 reservoirs as a function of pressure was developed using published experimental

552 studies. Jokhio and Tiab, (2002) method to construct and predict the IPR curves for
 553 gas condensate reservoirs was modified by using developed general viscosity
 554 correlation incorporated with two phase compressibility factor.

555 (2) The new IPR model developed based on assumption of transient fluid flow theory
 556 and superposition principle in calculating effective permeability integrals from
 557 pressure transient teste data.

558 (3) The validity of new IPR model was tested through compositional simulation on a field
 559 case (KAL-05) high temperature gas condensate well. The results of new IPR model
 560 compared with compositional simulation study and Jokhio and Tiab, (2002).The
 561 results showed that the new model outperform Jokhio and Tiab, (2002).

562 (4) The results of this study show that using single dry gas equation is not applicable for
 563 modelling gas condensate reservoir under depletion, where two phase flow exist.

564 (5) The new analytical approach in this study provides an appropriate engineering tool
 565 for uncertainty studies and decision making for choosing the best heavy gas
 566 condensate reservoir strategy.

567 (6) This simple analytical method can predict performance of gas condensate reservoirs,
 568 without requirement for expensive and time consuming computational simulation.

569 Appendix A

570 Procedure to calculate gas phase PVT Table 4

571 To calculate pseudocritical properties (pressure and temperature) equation of Sutton, (2005)
 572 Eq. (10) and Eq. (11) developed for gas condensate reservoir is used as follow:

$$T_{pc} = 164.3 + 357.7\gamma_g - 67.7\gamma_g^2$$

$$T_{pc} = 164.3 + 357.7(0.94) - 67.7(0.94)^2 = 440.72^\circ R$$

$$P_{pc} = 744 - 125.4\gamma_g + 5.9\gamma_g^2$$

$$P_{pc} = 744 - 125.4(0.94) + 5.9(0.94)^2 = 631.34 \text{ psia}$$

573 At 2600 psia

$$T_{pr} = \frac{T}{T_{pc}} = \frac{(354 + 460)}{440.72} = 1.846 \quad (\text{A1})$$

$$P_{pr} = \frac{P}{P_{pc}} = \frac{2600}{631.34} = 4.1182 \quad (\text{A2})$$

574 Using Eq. (9) to calculate two-phase compressibility factor.

$$Z_{2p} = A_0 + A_1(P_r) + A_2\left(\frac{1}{T_r}\right) + A_3(P_r)^2 + A_4\left(\frac{1}{T_r}\right)^2 + A_5\left(\frac{P_r}{T_r}\right)$$

$$Z_{2p} = 2.24353 + (0.0375281)(4.12) + (3.56539)\left(\frac{1}{1.846}\right) + 0.000829231(4.12)^2 \\ + 1.53428\left(\frac{1}{1.846}\right)^2 + 0.131987\left(\frac{4.12}{1.846}\right) = 0.91$$

$$Z_{2p} = 0.91$$

$$B_g = 0.00504 \frac{Z_{2p}T}{P} = 0.00504 \frac{(0.91)(354 + 460)}{2600} = 0.00144 \text{ bbl/SCF} \quad (\text{A3})$$

575 Use Eq. (6) to calculate gas density

$$\rho_g = 1.601846 \times 10^{-2} \frac{Mw.P}{RT}$$

$$\rho_g = 1.601846 \times 10^{-2} \frac{(27.17) \times (2600)}{(10.73)(354 + 460)} = 0.1296 \text{ g/cc}$$

576 Calculate gas viscosity at 2600psia use developed correlation, Eq. (8).

$$\mu_{gc} = 0.000246933K \exp \left[X \left(\frac{\rho_g}{27.6718} \right)^Y \right]$$

577 Where:

$$K = \frac{(16.7175 + 0.0419188M)T^{1.40256}}{212.209 + 18.1349M + T} = \frac{(16.7175 + 0.0419188 \times 27.17)(814)^{1.40256}}{212.209 + 18.1349(27.17) + 814} = 142.95$$

$$X = 2.12575 + \frac{2063.71}{T} + 0.011926M = 2.12575 + \frac{2063.71}{814} + 0.011926 \times 27.17 = 4.99$$

$$Y = 1.09809 - 0.0392581X = 1.09809 - 0.0392581 \times 4.99 = 0.902$$

$$\mu_{gc} = 0.000246933K \exp \left[X \left(\frac{\rho_g}{27.6718} \right)^Y \right] = 0.000246933(142.95) \times \exp \left[4.99 \left(\frac{0.1296}{27.6718} \right)^{0.902} \right] \\ = 0.03649 \text{ cp}$$

578 To calculate solution gas to oil ratio R_s , modified form of Kartoatmodjo and Schmidt, (1991)
579 is used.

$$R_s = (P^{1.1535}) \left(\frac{\gamma_g}{37.966} \right) \times 10^{\left(\frac{9.441API}{T} \right)} \quad (\text{A4})$$

580 Where T is in \mathcal{R}

$$R_s = (2600^{1.1535}) \left(\frac{0.94}{37.966} \right) \times 10^{\left(\frac{9.441 \times 50}{354 + 460} \right)} = 818.1233$$

581 Calculate oil to gas ratio, R_o [STB/MMscf], as follow:

$$R_o = -11.66 + 4.706 \times 10^{-9}(R_s)^3 + 1.623\sqrt{R_s} - \frac{42.3815}{\sqrt{R_s}}$$

$$R_o = -11.66 + 4.706 \times 10^{-9}(818.123)^3 + 1.623\sqrt{818.1233} - \frac{42.3815}{\sqrt{818.1233}} = 35.8576 \frac{STB}{MMscf} \\ = 3.58 \times 10^{-5} STB/scf$$

582 Producing gas to oil ratio, R_p was measured at the surface of the well during pressure
 583 transient test: $R_p=9470$ scf/STB. Table 3, is include PVT properties of gas phase for entire
 584 pressure range.

585 **Table 3**

586 PVT Properties for gas-phase in region 1.

| P (psia) | Ppr (psi) | Z _(Two-phase) | B _g (B/scf) | New Vis model, μ_g (cp) | Rs (scf/STB) |
|----------|-----------|--------------------------|------------------------|-----------------------------|--------------|
| 200 | 0.31 | 0.872 | 0.0179 | 0.0352 | 42.45 |
| 600 | 0.95 | 0.879 | 0.0060 | 0.0354 | 150.74 |
| 1000 | 1.58 | 0.885 | 0.0036 | 0.0356 | 271.73 |
| 1400 | 2.21 | 0.891 | 0.0026 | 0.0358 | 400.59 |
| 1800 | 2.85 | 0.898 | 0.0020 | 0.0360 | 535.30 |
| 2200 | 3.48 | 0.904 | 0.0016 | 0.0362 | 674.73 |
| 2600 | 4.11 | 0.910 | 0.0014 | 0.0364 | 818.12 |
| 3000 | 4.75 | 0.917 | 0.0012 | 0.0366 | 964.95 |
| 3400 | 5.38 | 0.923 | 0.0011 | 0.0368 | 1114.82 |
| 3800 | 6.01 | 0.930 | 0.0010 | 0.0370 | 1267.43 |
| 4200 | 6.65 | 0.936 | 0.0009 | 0.0372 | 1422.54 |
| 4600 | 7.28 | 0.942 | 0.0008 | 0.0374 | 1579.93 |
| 5000 | 7.91 | 0.9491 | 0.0007 | 0.0376 | 1739.43 |
| 5400 | 8.55 | 0.955 | 0.0007 | 0.0378 | 1900.91 |
| 5800 | 9.18 | 0.961 | 0.0006 | 0.0380 | 2064.24 |
| 6200 | 9.82 | 0.968 | 0.0006 | 0.0382 | 2229.31 |
| 6750 | 10.69 | 0.976 | 0.0005 | 0.0385 | 2458.94 |

587 Appendix B

588 Calculation of pseudopressure integral

589 In this section calculation step of two phase pseudopressure integral for gas phase is
 590 demonstrated, trapezoidal rule of integration was used to evaluate the integral. Eq. (24)

$$\Delta m P_{gt} = \left[\int_{p_{wf}}^{P_{avg}} \left(\frac{1}{B_{gd} \mu_g} \right) \frac{R_p (1 - R_o R_s)}{(R_p - R_s)} (P) dp \right] \times \int_{p_{wf}}^{P_{avg}} k \cdot k_{rg}(P) dp$$

591 First part of the integral is calculated as follow:

592 if, $X = \left(\frac{1}{B_{gd} \mu_g} \right) \frac{R_p (1 - R_o R_s)}{(R_p - R_s)}$, the pseudopressure integral can be written as follow:

$$\Delta m P_g = \int_{p_{wf}}^{P_{avg}} X(P) dp$$

593 Having calculated the PVT properties, at pressure of 200psia, (X_{200}) can be calculated as
 594 follow:

$$X_{200} = \left(\frac{1}{B_g \mu_g} \right) \frac{R_p(1 - R_o R_s)}{(R_p - R_s)} = \frac{9470 \times (1 - (-7.58E - 06 \times 42.45))}{(0.0179 \times 0.035) \times (9470 - 42.45)} = 1797.3$$

$$X_0 = 0$$

595 Hence:

$$\Delta m P_{gt} = \int_0^{200} X(P) dp$$

$$\int_0^{200} X(P) dp = \frac{0 + 1797.3}{2} (200 - 0) = 179730 \text{ psi}^2/cp$$

596 Second part of Eq. (24), is effective permeability integral that can be calculated as follow at
597 pressure 6574.3psia. Having calculated pseudopressure derivative group $(d\Delta m P_g)/d\ln(t)$,
598 effective permeability integral at 6574.3psia is

$$\int_{P_{wf}}^{P_{avg}} k_{rg}(6574.3) dp = 162.6 \frac{q_{g,meas}}{h \left(\frac{d\Delta m P_g}{d\ln(t)} \right)} = \frac{162.6}{44080.16} \frac{75.4 \times 100}{216.5} = 0.1283 \text{ cp}$$

599 Calculating several values of the effective permeability integral at various pressure, results in
600 constructing Fig. (10). The other pressure range of permeability integral can be estimated
601 from extrapolation of this graph. For pressure of 200psia the effective permeability integral is
602 0.000074.

603 Hence pseudopressure integral at 200psia, Eq. (24) is:

$$\Delta m P_g = 179730 \times 0.000074 = 13.3 \frac{\text{psi}^2}{cp} = 0.00001338 \text{ MM} \frac{\text{psi}^2}{cp}$$

604 And continue the above procedure for given bottom-hole flowing pressures.

605 The result of pseudopressure, pseudopressure derivative group and effective permeability
606 integral is presented in Table 4.

607 **Table 4**

608 Pressure, pseudopressure and pseudopressure derivative results, for gas-phase.

| Time(hours) | P(psia) | m(p),region gas | Δm_p , MMpsi ² /cp | t. $\Delta m P/d(\ln(t))$ | Integral (Keg) |
|-------------|---------|--------------------|--|---------------------------|----------------|
| 0 | 1083.1 | 24674.74 | | | |
| 0.167 | 1174.5 | 26844.29 | 3647.32 | | |
| 0.333 | 1226.7 | 30147.45 | 5816.87 | | |
| 0.5 | 1303.6 | 38660.77 | 9120.02 | 7916.19 | |
| 1 | 1490.6 | 51522.34 | 17633.34 | 12347.16 | |
| 2 | 1751.6 | 67104.64 | 30494.91 | 29919.68 | |
| 3 | 2046 | 80061.04 | 46077.22 | 39009.35 | |

| | | | | | |
|-----|--------|-----------|-----------|-----------|--------|
| 4 | 2279.4 | 107613.27 | 59033.61 | 56001.64 | |
| 6 | 2759.4 | 136008.52 | 86585.84 | 76609.43 | |
| 8 | 3246.5 | 189821.83 | 114981.09 | 108816.41 | |
| 12 | 4210 | 236758.29 | 168794.41 | 145354.52 | |
| 16 | 5162 | 276446.10 | 215730.86 | 145893.57 | |
| 22 | 6161 | 282294.79 | 255418.67 | 100093.52 | |
| 28 | 6336.5 | 284516.45 | 261267.37 | 63915.29 | 0.0088 |
| 34 | 6406.1 | 285966.50 | 263489.02 | 18041.50 | 0.0313 |
| 42 | 6452.5 | 287037.70 | 264939.07 | 10466.39 | 0.0541 |
| 50 | 6487.3 | 287665.09 | 266010.27 | 6400.52 | 0.0884 |
| 58 | 6507.6 | 288227.53 | 266628.66 | 5838.47 | 0.0969 |
| 68 | 6526.5 | 289137.98 | 267200.10 | 5438.58 | 0.1041 |
| 82 | 6556.9 | 289654.26 | 268110.55 | 4062.96 | 0.1393 |
| 97 | 6574.3 | 290037.67 | 268626.83 | 4408.16 | 0.1284 |
| 112 | 6587.3 | 29.463.04 | 269010.26 | 3114.06 | 0.1818 |
| 141 | 6601.8 | 21027.43 | 269435.62 | | |

609

610 Appendix C

611 Procedure to calculate condensate (oil) PVT

612 Calculate the PVT for condensate part, estimate P_{pc} by Eq. (10) and T_{pc} by Eq. (11) as
613 follow:

$$P_{pc} = 744 - 125.4\gamma_{condensate} + 5.9\gamma_{condensate}^2$$

$$T_{pc} = 164.3 + 357.7\gamma_{condensate} - 67.7\gamma_{condensate}^2$$

614 Where specific gravity of condensate $\gamma_{condensate}$ is calculated from the following equation:

$$\gamma_o = \frac{141.5}{131.5 + API} = \frac{141.5}{131.5 + 50} = 0.779 \quad (C1)$$

615 Hence:

$$P_{pc} = 744 - 125.4(0.779) + 5.9(0.779)^2 = 649.9$$

$$T_{pc} = 164.3 + 357.7(0.779) - 67.7(0.779)^2 = 402.02$$

616 P_{pr} and T_{pr} at pressure of 2200 psia are as follow:

$$P_{pr} = \frac{P}{P_{pc}} = \frac{2200}{649.9} = 3.385$$

$$T_{pr} = \frac{T}{402.02} = \frac{(354 + 460)}{402.02} = 2.025$$

617 To evaluate compressibility factor of condensate phase, Eq. (9) is used. Having calculated

618 P_{pr} and T_{pr} at pressure of 2200psia, compressibility is calculated as follow:

$$Z_{2p} = A_0 + A_1(P_{pr}) + A_2\left(\frac{1}{T_{pr}}\right) + A_3(P_{pr})^2 + A_4\left(\frac{1}{T_{pr}}\right)^2 + A_5\left(\frac{P_{pr}}{T_{pr}}\right)$$

$$Z_{2p} = 2.2435 - (0.03752)(3.385) + 3.5653 \left(\frac{1}{2.025} \right) + 0.000829(3.385)^2 + 1.5342 \left(\frac{1}{2.025} \right)^2 + 0.131987 \left(\frac{3.385}{2.025} \right) = 0.96$$

619 Standing and Katz, (1942) correlation is used to calculate condensate (oil) formation volume
620 factor. At pressure of 2600psia.

$$B_o = 0.972 + 0.000147F^{1.175} \quad (C2)$$

621 Where:

$$F = R_s \left(\frac{Y_g}{Y_o} \right)^{0.5} + 1.25T, \quad T = ^\circ F \quad (C3)$$

622 In equation C3, R_s is determined by modified correlation of Kartoatmodjo and Schmidt,
623 (1991) as follow:

$$R_s = (P^{1.1535}) \left(\frac{Y_g}{37.966} \right) \times 10^{\left(\frac{9.441API}{T} \right)} \quad (C4)$$

624 Where T is \mathcal{R}

$$R_s = (2600^{1.1535}) \left(\frac{0.94}{37.966} \right) \times 10^{\left(\frac{9.441 \times 50}{354 + 460} \right)} = 678.53$$

625 Therefore:

$$F = 678.63 \times \left(\frac{0.94}{0.779614} \right)^{0.5} + 1.25 \times (354) = 1187.7$$

$$B_o = 0.972 + 0.000147(1187.7)^{1.175} = 1.5746$$

626 To estimate the oil to gas ratio the following equation is used:

$$R_o = -11.66 + 4.706 \times 10^{-9}(R_s)^3 + 16.623\sqrt{R_s} - \frac{42.3815}{\sqrt{R_s}} \quad (C5)$$

627 At 2600psia:

$$R_o = -11.66 + 4.706 \times 10^{-9}(678.53)^3 + 16.623\sqrt{678.53} - \frac{42.3815}{\sqrt{678.53}} = 3.046 \times 10^{-5} STB/scf$$

628 To estimate the viscosity of condensate phase, modified form of Beggs and Robinson,
629 (1975), Eq. (C5) is used. For dead oil viscosity modified Egbogah and Jack, (1990)
630 correlation shown in Eq. (C10) is used.

$$\mu_c = (25.1921(R_s + 100)^{-0.6487})\mu_{od}[2.7516(R_s + 150)^{-0.2135}] \quad (C6)$$

$$\log. \log(\mu_{od} + 1) = 1.8513 - 0.0255484API - 0.56238 \log(Tg) \quad (C7)$$

631 API assumed to be 50 in this study. Damaged skin factor is taken as -4.1235 after Jokhio
632 and Tiab (2002).

633 Table 5 depicts the PVT results of condensate phase.

638

639 **Table 5**

640 PVT properties of condensate (oil) phase.

| P | Ppr (psi) | $Z_{(Two-phase)}$ | Bo (B/scf) | Vis, μ_o (cp) | Rs (scf/STB) | Ro(STB/scf) |
|------|-----------|-------------------|------------|-------------------|--------------|-------------|
| 200 | 0.3077 | 0.8654 | 1.1804 | 0.2825 | 35.2076 | -9.1722E-06 |
| 600 | 0.9233 | 0.8831 | 1.2315 | 0.1866 | 125.0248 | 2.7064E-06 |
| 1000 | 1.5388 | 0.9014 | 1.2903 | 0.1374 | 225.3714 | 9.9359E-06 |
| 1400 | 2.1544 | 0.9203 | 1.3549 | 0.1083 | 332.2443 | 1.5771E-05 |
| 1800 | 2.7699 | 0.9398 | 1.4241 | 0.0893 | 443.9722 | 2.0938E-05 |
| 2200 | 3.3855 | 0.9600 | 1.4975 | 0.0758 | 559.6075 | 2.5767E-05 |
| 2600 | 4.0010 | 0.9808 | 1.5746 | 0.0659 | 678.5326 | 3.046E-05 |
| 3000 | 4.6166 | 1.0022 | 1.6551 | 0.0582 | 800.3101 | 3.5168E-05 |
| 3400 | 5.2321 | 1.0243 | 1.7387 | 0.0521 | 924.6128 | 4.0017E-05 |
| 3800 | 5.8477 | 1.0469 | 1.8253 | 0.0472 | 1051.1854 | 4.512E-05 |
| 4200 | 6.4633 | 1.07029 | 1.9147 | 0.0431 | 1179.8234 | 5.0582E-05 |
| 4600 | 7.0788 | 1.0942 | 2.0067 | 0.0397 | 1310.3585 | 5.6508E-05 |
| 5000 | 7.6944 | 1.1187 | 2.1012 | 0.0367 | 1442.6496 | 6.2999E-05 |
| 5400 | 8.3099 | 1.1439 | 2.1980 | 0.0342 | 1576.5769 | 7.0157E-05 |
| 5800 | 8.9255 | 1.1698 | 2.2972 | 0.0320 | 1712.037 | 7.8085E-05 |
| 6200 | 9.5410 | 1.1962 | 2.3985 | 0.0301 | 1848.9398 | 8.6888E-05 |
| 6750 | 10.38 | 1.2336 | 2.5413 | 0.0278 | 2039.3927 | 0.00010061 |

641

642 **References**

643 Ahmed, T.H., 2010. Reservoir engineering handbook, 4th ed. Gulf Professional Pub, Oxford.

644 Al-Hussainy, R., Ramey, H.J., Crawford, P.B., 1966. The Flow of Real Gases Through
645 Porous Media. J. Pet. Technol. 18, 624–636. <https://doi.org/10.2118/1243-A-PA>646 Al-Meshari, A., Kokal, S., Al-Muhainy, A., Ali, M., 2007. Measurement of Gas Condensate,
647 Near-Critical and Volatile Oil Densities and Viscosities at Reservoir Conditions, in:
648 Proceedings of SPE Annual Technical Conference and Exhibition. Society of Petroleum
649 Engineers, California. <https://doi.org/10.2523/108434-ms>650 Al-Nasser, K.S., Al-Marhoun, M.A., 2012. Development of New Gas Viscosity Correlations,
651 in: SPE International Production and Operations Conference & Exhibition. Society of
652 Petroleum Engineers, Doha. <https://doi.org/10.2118/153239-ms>653 Arukhe, I.N., Mason, W.E., 2012. The Use of Two Phase Compressibility Factors in
654 Predicting Gas Condensate Performance, in: SPE Annual Technical Conference and
655 Exhibition. Society of Petroleum Engineers, San Antonio.
656 <https://doi.org/10.2118/159080-ms>

- 657 Beggs, H.D., Robinson, J.R., 1975. Estimating the Viscosity of Crude Oil Systems. *J. Pet.*
658 *Technol.* 27, 1140–1141. <https://doi.org/10.2118/5434-PA>
- 659 Behmanesh, H., Hamdi, H., Clarkson, C.R., 2017. Production data analysis of gas
660 condensate reservoirs using two-phase viscosity and two-phase compressibility. *J. Nat.*
661 *Gas Sci. Eng.* 47, 47–58. <https://doi.org/10.1016/j.jngse.2017.07.035>
- 662 Bonyadi, M., Rahimpour, M.R., Esmailzadeh, F., 2012. A new fast technique for calculation
663 of gas condensate well productivity by using pseudopressure method. *J. Nat. Gas Sci.*
664 *Eng.* 4, 35–43. <https://doi.org/10.1016/J.JNGSE.2011.07.012>
- 665 Bonyadi, M., Rostami, M., 2017. A new viscosity model based on Soave-Redlich-Kwong
666 equation of state. *Fluid Phase Equilib.* 451, 40–47.
667 <https://doi.org/10.1016/J.FLUID.2017.07.009>
- 668 Chen, H.L., Wilson, S.D., Monger-McClure, T.G., 1995. Determination of Relative
669 Permeability and Recovery for North Sea Gas Condensate Reservoirs, in: *SPE Annual*
670 *Technical Conference and Exhibition*. Society of Petroleum Engineers, Dallas.
671 <https://doi.org/10.2118/30769-MS>
- 672 Dake, L.P., 2001. *The practice of reservoir engineering*, 3rd ed. Elsevier, Amsterdam.
- 673 Davani, E., Falcone, G., Teodoriu, C., McCain, W.D., 2013. HPHT viscosities measurements
674 of mixtures of methane/nitrogen and methane/carbon dioxide. *J. Nat. Gas Sci. Eng.* 12,
675 43–55. <https://doi.org/10.1016/J.JNGSE.2013.01.005>
- 676 Earlougher, R.C., 1977. *Advances in well test analysis*. SPE.
- 677 Economides, M.J., Cikes, M., Pforter, H., Udick, T.H., Uroda, P., 1989. The Stimulation of a
678 Tight, Very-High- Temperature Gas-Condensate Well. *SPE Form. Eval.* 4, 63–72.
679 <https://doi.org/10.2118/15239-PA>
- 680 Economides, M.J., Cikes, M., Udick, T.H., Uroda, P., 1989. The Stimulation of a Tight , Very-
681 High- Temperature Gas-Condensate Well. *SPE Form. Eval.* Economides, 63–72.
- 682 Egbogah, E., Jack, N., 1990. An improved temperature-viscosity correlation for crude oil
683 systems. *J. Pet. Sci. Eng.* 5, 197–200.
- 684 Elsharkawy, A.M., 2006. Efficient methods for calculations of compressibility, density, and
685 viscosity of natural gases, in: *Journal of Canadian Petroleum Technology*. Petroleum
686 Society of Canada, pp. 55–61. <https://doi.org/10.2118/06-06-04>
- 687 Elsharkawy, A.M., Hashem, Y.S.K.S., Alikhan, A.A., 2000. Compressibility Factor for Gas
688 Condensates, in: *SPE Permian Basin Oil and Gas Recovery Conference*. Society of

- 689 Petroleum Engineers, Midland. <https://doi.org/10.2118/59702-MS>
- 690 Evinger, H.H., Muskat, M., 1942. Calculation of Theoretical Productivity Factor. *Trans. AIME*
691 146, 126–139. <https://doi.org/10.2118/942126-g>
- 692 Fattah, K.A., Elias, M., El-Banbi, H.A., El-Tayeb, E.-S.A., 2014. New Inflow Performance
693 Relationship for solution-gas drive oil reservoirs. *J. Pet. Sci. Eng.* 122, 280–289.
694 <https://doi.org/10.1016/j.petrol.2014.07.021>
- 695 Fetkovich, M.D., Guerrero, E.T., Of Tulsa, U., Fetkovich, M.J., Thomas, L.K., 1986. SPE Oil
696 and Gas Relative Permeabilities Determined From Rate-Time Performance Data.
697 Society of Petroleum Engineers, New Orleans.
- 698 Fevang, Ø., 1995. Gas Condensate Flow Behavior and Sampling, October.
- 699 Fevang, Ø., Whitson, C.H., 1996. Modeling Gas-Condensate Well Deliverability. *SPE*
700 *Reserv. Eng.* 11, 221–230. <https://doi.org/10.2118/30714-PA>
- 701 Gilbert, W.E., 1954. Flowing and gas-lift well performance, in: *API Drilling and Production*
702 *Practice*. American Petroleum Institute, Los Angeles. <https://doi.org/10.2118>
- 703 Gondouin, M., Iffly, R., Husson, J., 1967. An Attempt to Predict the Time Dependence of
704 Well Deliverability in Gas Condensate Fields. *Soc. Pet. Eng. J.* 7, 113–124.
705 <https://doi.org/10.2118/1478-pa>
- 706 Guehria, F.M., 2000. Inflow Performance Relationships for Gas Condensates, in: *SPE*
707 *Annual Technical Conference and Exhibition*. Society of Petroleum Engineers.
708 <https://doi.org/10.2118/63158-MS>
- 709 Guo, B., Sun, K., Ghalambor, A., 2008. Well Productivity Handbook: Vertical, Fractured,
710 Horizontal, Multilateral, and Intelligent Wells, 1st ed, *Well Productivity Handbook:*
711 *Vertical, Fractured, Horizontal, Multilateral, and Intelligent Wells*. Gulf Publishing
712 Company, Suite. <https://doi.org/10.1016/C2013-0-15529-8>
- 713 Hekmatzadeh, M., Gerami, S., 2018. A new fast approach for well production prediction in
714 gas-condensate reservoirs. *J. Pet. Sci. Eng.* 160, 47–59.
715 <https://doi.org/10.1016/j.petrol.2017.10.032>
- 716 Hernandez, J.C., Vesovic, V., Carter, J.N., Lopez, E., 2002. Sensitivity of Reservoir
717 Simulations to Uncertainties in Viscosity, in: *SPE/DOE Improved Oil Recovery*
718 *Symposium*. Society of Petroleum Engineers, Oklahoma. <https://doi.org/10.2118/75227->
719 [ms](https://doi.org/10.2118/75227-ms)
- 720 Horner, D.R., 1951. Pressure Build-up in Wells, in: *3rd World Petroleum Congress*. World

- 721 Petroleum Congress, The Hague.
- 722 Jokhio, S.A., Tiab, D., 2002. Establishing Inflow Performance Relationship (IPR) for Gas
723 Condensate Wells, in: SPE Gas Technology Symposium. Society of Petroleum
724 Engineers, Alberta, pp. 1–20. <https://doi.org/10.2118/75503-MS>
- 725 Jokhio, S.A., Tiab, D., Escobar, F., 2002. Forecasting Liquid Condensate and Water
726 Production In Two-Phase And Three-Phase Gas Condensate Systems. Society of
727 Petroleum Engineers, San Antonio, pp. 1–13. <https://doi.org/10.2118/77549-ms>
- 728 Kartoatmodjo, T.R.S., Schmidt, Z., 1991. New Correlations For Crude Oil Physical
729 Properties.
- 730 Kniazeff, V.J., Naville, S.A., 1965. Two-Phase Flow of Volatile Hydrocarbons. Soc. Pet. Eng.
731 J. 5, 37–44. <https://doi.org/10.2118/962-pa>
- 732 Lee, A.L., Gonzalez, M.H., Eakin, B.E., 1966. The Viscosity of Natural Gases. J. Pet.
733 Technol. 18, 997–1000. <https://doi.org/10.2118/1340-PA>
- 734 Ling, K., McCain, W.D., Davani, E., Falcone, G., 2009. Measurement of Gas Viscosity at
735 High Pressures and High Temperatures, in: International Petroleum Technology
736 Conference. International Petroleum Technology Conference, Doha.
737 <https://doi.org/10.2523/iptc-13528-ms>
- 738 Lohrenz, J., Bray, B.G., Clark, C.R., 1964. Calculating Viscosities of Reservoir Fluids From
739 Their Compositions. J. Pet. Technol. 16, 1171–1176. <https://doi.org/10.2118/915-PA>
- 740 Londono, F.E., Archer, R.A., Blasingame, T.A., 2002. Correlations for Hydrocarbon Gas
741 Viscosity and Gas Density - Validation and Correlation of Behavior Using a Large-Scale
742 Database. SPE Reserv. Eval. Eng. 8, 561–572. <https://doi.org/10.2118/75721-pa>
- 743 Lyons, W.C., Pilsga, G.J., Lorenz, M.D., 2016. Standard handbook of petroleum and natural
744 gas engineering, Third. ed. Gulf Professional Publishing, Oxford.
- 745 McCain, W.D., Cawley, G., 1991. Reservoir-Fluid Property Correlations-State of the Art. SPE
746 Reserv. Eng. 6, 266–272. <https://doi.org/10.2118/18571-pa>
- 747 Mott, R., 2003. Engineering Calculations of Gas-Condensate-Well Productivity. SPE Reserv.
748 Eval. Eng. 6, 298–306. <https://doi.org/10.2118/86298-PA>
- 749 O'Dell, H., Miller, R., 1967. Successfully Cycling a Low-Permeability, High-Yield Gas
750 Condensate Reservoir. J. Pet. Technol. 19, 41–47. <https://doi.org/10.2118/1495-PA>
- 751 Penula, G., 2003. Gas-Condensate Well-Test Analysis with and without the Relative

- 752 Permeability Curves, in: Annual Technical Conference and Exhibition Held in Dallas.
753 SPE, Dallas. <https://doi.org/10.1306/a9673950-1738-11d7-8645000102c1865d>
- 754 Piper, L.D., W.D., M., Corredor, J.H., 1993. Compressibility Factors for Naturally Occurring
755 Petroleum Gases, in: SPE Annual Technical Conference and Exhibition. Society of
756 Petroleum Engineers, Houston. <https://doi.org/10.2523/26668-ms>
- 757 Qasem, F., Gharbi, R., Baroon, B., 2014. IPR in Naturally Fractured Gas Condensate
758 Reservoirs, in: SPE Latin America and Caribbean Petroleum Engineering Conference.
759 Society of Petroleum Engineers, pp. 21–23. <https://doi.org/10.2118/169286-MS>
- 760 Rahimzadeh, A., Bazargan, M., Darvishi, R., Mohammadi, A.H., 2016. Condensate blockage
761 study in gas condensate reservoir. *J. Nat. Gas Sci. Eng.* 33, 634–643.
762 <https://doi.org/10.1016/J.JNGSE.2016.05.048>
- 763 Rawlins, E., Schellhardt, M., 1936. Back-Pressure Data on Natural Gas Wells and Their
764 Application to Production Practices, in: Bureau of Mines Monograph. Bureau of Mines
765 Monograph.
- 766 Rayes, D.G., Piper, L.D., McCain, W.D., Poston, S.W., 1992. Two-Phase Compressibility
767 Factors for Retrograde Gases. *SPE Form. Eval.* 7, 87–92.
768 <https://doi.org/10.2118/20055-PA>
- 769 Roussennac, B., 2001. Gas condensate well test analysis. *Dep. Pet. Eng.* Stanford
770 University.
- 771 Serra, K., Peres, A.M., Reynolds, A.C., 1990. Well-Test Analysis for Solution-Gas-Drive
772 Reservoirs: Part 1-Determination of Relative and Absolute Permeabilities. *SPE Form.*
773 *Eval.* 05, 124–132.
- 774 Serra, K. V., Peres, A.M.M., Reynolds, A.C., 2007. Well-Test Analysis for Solution-Gas-Drive
775 Reservoirs: Part 2-Buildup Analysis. *SPE Form. Eval.* 5, 133–140.
776 <https://doi.org/10.2118/17048-pa>
- 777 Shahamat, M.S., Tabatabaie, S.H., Mattar, L., Motamed, E., 2015. Inflow Performance
778 Relationship for Unconventional Reservoirs (Transient IPR), in: SPE/CSUR
779 Unconventional Resources Conference. Society of Petroleum Engineers, Calgary.
780 <https://doi.org/10.2118/175975-MS>
- 781 Sousa, P.C. De, Garcia, A.P., Waltrich, P.J., 2017. Analytical Development of a Dynamic
782 IPR for Transient Two-Phase Flow in Reservoirs, in: SPE Annual Technical Conference
783 and Exhibition. Society of Petroleum Engineers, San Antonio.

- 784 <https://doi.org/10.2118/187232-MS>
- 785 Standing, M.B., Katz, D.L., 1942. Density of Natural Gases. *Trans. AIME* 146, 140–149.
- 786 <https://doi.org/10.2118/942140-g>
- 787 Stewart, G., 2012. *Wireline Formation Testing and Well Deliverability : With Complex*
- 788 *Reservoir Material Balance.*, 1st ed. PennWell Corporation, Tulsa.
- 789 Stewart, G., 2011. *Well Test Design and Analysis.* PennWell Corporation, Tulsa.
- 790 Sutton, R.P., 2005. Fundamental PVT Calculations for Associated and Gas/Condensate
- 791 Natural-Gas Systems. *SPE Reserv. Eval. Eng.* 10, 270–284.
- 792 <https://doi.org/10.2118/97099-pa>
- 793 Sutton, R.P., 1985. Compressibility Factors for High-Molecular-Weight Reservoir Gases, in:
- 794 *SPE Annual Technical Conference and Exhibition.* Society of Petroleum Engineers, Las
- 795 Vegas. <https://doi.org/10.2118/14265-ms>
- 796 Thomas, F.B., Bennion, D.B., 2009. Gas Condensate Reservoir Performance. *J. Can. Pet.*
- 797 *Technol.* 10.
- 798 Wheaton, R.J., Zhang, H.R., 2007. Condensate Banking Dynamics in Gas Condensate
- 799 Fields: Compositional Changes and Condensate Accumulation Around Production
- 800 Wells. <https://doi.org/10.2118/62930-ms>
- 801 Whitson, C., W, J., Brulé, M., 2000. *Phase Behavior*, 1st ed, Society. Society of Petroleum
- 802 Engineers. <https://doi.org/10.1021/ma00080a014>
- 803 Whitson, C.H., Fevang, Ø., Yang, T., 1999. Gas Condensate PVT – What’s Really Important
- 804 and Why?, in: *Optimisation of Gas Condensate Fields.* Norwegian U. of Science and
- 805 Technology, London. <https://doi.org/10.2118/117930-PA>
- 806 Yang, T., Fevang, O., Christoffersen, K., Ivarrud, E., 2007. LBC Viscosity Modeling of Gas
- 807 Condensate to Heavy Oil, in: *SPE Annual Technical Conference and Exhibition.* Society
- 808 of Petroleum Engineers, Anaheim. <https://doi.org/10.2523/109892-ms>
- 809 Yu, X., Lei, S., Liangtian, S., Shilun, L., 1996. A New Method for Predicting the Law of
- 810 Unsteady Flow Through Porous Medium on Gas Condensate Well, in: *SPE Gas*
- 811 *Technology Symposium.* Society of Petroleum Engineers, Calgary.
- 812 <https://doi.org/10.2118/35649-ms>

813

- New gas condensate viscosity correlation developed
- Inflow Performance Relationship curves are established for high temperature gas condensate reservoirs
- Multi-flash compositional simulation of a high temperature gas condensate well performed
- Pressure transient test data utilized to evaluate effective permeability integral
- Pseudopressure function is used to model gas condensate reservoir performance